S1. PMF Analysis of AMS NR HR-Org and AMS NR HR-SO_4

Positive matrix factorization of high resolution (HR) organic (Org) and sulfate (SO_4) AMS data was performed using the PMF Evaluation Tool, PET (Ulbrich et al., 2009). Ion fragments with low signal-to-noise (SNR) were downweighted ($0.2 < SNR < 2$) by a factor of 2 or removed ($SNR < 0.2$). Ion fragments associated with m/z 44 (CO_2^+, CO^+, H_2O^+, HO^+, O^+) were also downweighted by a factor of 2. No data smoothing or spike removal was applied to the matrices.

Fit quality (Q/Q_{exp}) and uncentered correlations were used to identify the best number of factors. Q/Q_{exp} decreases with an increasing number of factors as each factor introduces an additional degree of freedom. Solutions with numbers of factors that resolve Q/Q_{exp} near a value of 1 is ideal such that an increased distance of Q/Q_{exp} from 1 is used as one of the criteria for rejecting a solution.

The 1 to 7 factor solutions and criteria of PMF analysis are summarized in Tables S1-4. Both "OminusC" and "Diff" data types were used for PMF analysis. The Diff data type is obtained by fitting the raw difference spectra while the OminusC data type is obtained by subtracting the "Open" ion sticks from the "Closed" ion sticks after peak fitting. The HR Diff Sticks data type was chosen due to its low absolute residual when compared to the HR OminusC Sticks data type. The OminusC data type had also produced solutions with high Q/Q_{exp} values, indicating that the errors associated with the input data have been underestimated.

The highest number of factors with no temporal nor spectral correlations was the final number of factors chosen as a solution for each period. A 3-factor solution with a Q/Q_{exp} value of 0.73 was chosen for marine periods during Autumn as the 4-factor solution produced an additional factor with a very similar spectrum ($R > 0.8$) to a factor identified in both the 3- & 4-factor solutions. A 2-factor solution with a Q/Q_{exp} value of 2.41 was selected for continental periods during Autumn. A 2-factor solution with a Q/Q_{exp} value of 0.51 was selected for marine periods during Early Spring. A 2-factor solution with a Q/Q_{exp} value of 0.34 was selected for continental periods during Early Spring. Only 1 factor in the 3-factor solution made up less than 10% of the total mass for marine periods during Autumn. For all other time periods, each factor made up more than 10% of the total mass.

The 2-3 resulting factors included a combination of a low-volatility oxidized organic aerosol (LVOOA) factor, a Sulfate factor, and an Amine factor. The mass spectra and time series of each factor are available in Figures S1-S5, and Table S5 shows the average mass concentrations.

The mass spectrum of the LVOOA factor shows prominent peaks at m/z 28 (CO^+), m/z 43 ($C_2H_3O^+$) and m/z 44 (CO_2^+), which are attributed to oxidized organic fragments (CHO1 and CHOgt1 AMS families). A high ratio of m/z 44/43, also evident of SOA oxidation, is used to identify the LVOOA factor as well as comparisons to previously reported LVOOA factors (Crippa et al., 2013;Hu et al., 2013;Ng et al., 2010;Hayes et al., 2013). This factor was present throughout Autumn but absent during Early Spring when there was also less continental

transport of AMS NR amine fragments. During continental periods in Autumn, this factor had the highest mass concentration but also the most variability (995 ± 1602 ng m^{-3}).

The Sulfate factor was found within all air masses and seasons and contained sulfate peaks at m/z 48 (SO^+), m/z 64 ($SO2^+$), m/z 80 (SO_3^+), m/z 81 (HSO_3^+), m/z 96 (SO_4^+), and m/z 98 ($H_2SO_4^+$) as well as organic peaks that are characteristic of particle aging at m/z 28 (CO^+) and m/z 44 (CO_2^+) in its mass spectrum. Larger organic peaks were present in continental air masses and during Autumn. Mass concentrations of the Sulfate factor were higher during continental periods than during marine periods and in Early Spring than in Autumn. The highest mass concentration of the Sulfate factor was observed during continental periods in Early Spring (609 ± 376 ng m^{-3}). With the exception of continental periods in Autumn, the Sulfate factor had the highest mass concentration among all the factors.

The final factor resolved during NAAMES was the Amine factor. This factor's mass spectrum consisted of both sulfate (m/z 48, m/z 64) and organic fragments, namely m/z 28 (CO^+) and m/z 44 (CO_2^+) which were of similar intensities. This factor is further characterized by a large, peak at m/z 73 ($C_3H_7NO^+$, $C_2H_5N_2O^+$), analogous to an oxidized amine ion fragment. This peak had the highest intensity for marine air masses in Autumn. Alternatively, oxidized organic peaks (m/z 28, m/z 44) had higher intensities during Early Spring. An unoxidized peak of a parent amine is seen at m/z 63 (C_4HN^+) for only marine air masses in Autumn (Qi et al., 2022). Interestingly, this factor was not observed during continental periods in Autumn. The highest mass concentration observed for the Amine factor was during continental periods in Early Spring (51 ± 90 ng m^{-3}). Overall, the Amine factor accounted for the lowest observed mass concentrations among all factors.

It is likely that a lack of organic mass during Early Spring resulted in no LVOOA factor and a smaller organic ion signal for the Sulfate factor for both marine and continental air masses. The Amine factor was very noisy, exhibiting high variability in mass concentration (±34-90 ng m^{-3}) that was nearly twice that of its mean (±17-51 ng m^{-3}). The noisiness of the time series of the Amine factor meant that it did not yield any useful source information for AMS NR amine fragments.

S2. AMS NR Single Particle Amine Fragments

AMS NR single particle amine fragments were estimated from the sum of 29 ions ($\Sigma CHN = CHN^+ + CH_3N^+ + CH_4N^+ + C_2H_3N^+ + C_2H_4N^+ + CHNO^+ + C_2H_5N^+ + C_2H_6N^+ + C_2H_4NO^+ C_3H_8N^+ + C_2H_5NO^+ + C_3H_9N^+ + CH_4N^+ + C_3H_6NO^+ + C_4H_{10}N^+ + C_2H_3NO_2^+ + C_2H_5N_2O^+ + C_3H_7NO^+ + C_4H_{11}N^+ + C_4H_6NO^+ + C_5H_{10}N^+ + C_4H_7NO^+ + C_5H_{11}N^+ + C_4H_8NO^+ + C_5H_{12}N^+ + C_4H_8N_2O^+ + C_5H_{10}NO^+ + C_6H_{14}N^+ + C_6H_{15}N^+$) to approximate amine within ET single particle measurements. Both unoxidized and oxidized amine ion fragments and ion fragments of parent amines are included. The average mass concentration and standard deviation of AMS NR single particle amine fragments in both marine and continental air masses during Autumn and Early Spring are shown in Table S6. Mass concentrations of AMS NR single particle amine fragments during marine periods were equivalent for both seasons but higher in Autumn than in Early Spring for continental air masses. The average mass concentration was also higher during marine periods in Early Spring but lower during marine periods in Autumn,

similar to the trend in mass concentrations seen for AMS NR amine fragments estimated by $C_xH_yN_z$ ion fragments.

Figure S6 displays the differences and similarities in the selection of AMS NR single particle amine fragments compared to the selection of AMS NR amine fragments. Both AMS NR single particle amine fragments and AMS NR amine fragments have little variability when regressed against FTIR NV amine groups in Early Spring and display a nearly vertical slope with p-values of 0.26 and 0.66, respectively. During Autumn, AMS NR single particle amine fragments and AMS NR amine fragments both display a strong correlation ($R = 0.87$) to FTIR NV amine groups. The p-values of these correlations are 0.95 for the former and 0.08 for the latter. While each of the four correlations is not statistically significant ($p > 0.05$), the overall p-value is lower when using AMS NR amine fragments rather than AMS NR single particle amine fragments. This shows that the sum of AMS NR amine fragments is less variable than the sum of AMS NR single particle amine fragments. Therefore, AMS NR amine fragments likely have more similarity to FTIR NV amine groups than the AMS NR single particle amine fragments, consistent with the expectation that the single particle signals are less accurate because of their lower m/z resolution and lower fragment specificity.

The ten AMS NR single particle amine fragments with the highest mass concentrations were CHN^+, CH_4N^+, $C_2H_3N^+$, $C_2H_4N^+$, $CHNO^+$, $C_2H_5N^+$, $C_2H_6N^+$, C_4HN^+, $C_2H_5N_2O^+$, $C_3H_7NO^+$. The presence of m/z 73 ($C_2H_5N_2O^+$, $C_3H_7NO^+$) in a mass spectrum is indicative of biomass burning, yet the concentration of these fragments remained largely constant across all periods. This either suggests that these fragments may come from a non-continental source or that a continental influence is present even for marine air masses. Figure S7 shows the variability of these low-molecular-weight ion fragments across marine and continental periods in Autumn and Early Spring. The average mass was highest during continental periods in Autumn for CHN^+, CH_4N^+, $C_2H_3N^+$, $C_2H_4N^+$, $CHNO^+$, $C_2H_5N^+$, $C_2H_6N^+$, $C_2H_5N_2O^+$, and $C_3H_7NO^+$. For C_4HN^+, the highest mass concentration was recorded during marine periods in Autumn. The average mass was lowest during marine periods in Autumn for CHN^+, $C_2H_4N^+$, $CHNO^+$, $C_2H_5N^+$, and $C_2H_6N^+$, during marine periods in Early Spring for $C_2H_3N^+$ and C_4HN^+, and during continental periods in Early Spring for CH_4N^+, $C_2H_5N_2O^+$, and $C_3H_7NO^+$.

The average fraction of total ion signal that each AMS NR single particle amine fragment contributes to its respective m/z is given in Table S7. While some AMS NR single particle fragments accounted for a greater portion of the average mass concentration, additional non-AMS NR single particle amine fragments that were fitted to the same m/z had dominated the signal, leading to a smaller fraction of the signal being apportioned to AMS NR single particle amine fragments. In Autumn, the fractions of AMS NR single particle amine fragments during marine periods were greater than during continental periods. In Early Spring, 8 of the 29 AMS NR single particle amine fragments accounted for a lower fraction of the ion signal in continental air masses than in marine air masses.

S3. ET Single Particle Analysis

The event trigger (ET) mode of the HR-ToF-AMS used three regions of interest (ROI) corresponding to a range of m/z to identify a single particle event and extract a mass spectrum.

These regions were set to m/z 43 (ROI1) with an event trigger level of 3.5 ions/extraction, m/z 55–79 (ROI2) with an event trigger level of 8 ions/extraction, and m/z 48-150 (ROI3) with an event trigger level of 9 ions/extraction. ROI1 could be triggered by rBC- and organic-containing particles hydrocarbon while ROI2 and ROI3 was set to identify aerosol components including nitrate, sulfate and organic. The single particle measurements were initially pre-processed using Tofware version 2.5.10 to generate input data for Cluster Input Preparation Panel (CIPP) version 2.1b which is used to identify real particles. Cluster Analysis Panel (CAP) version 2.1a (developed by Alex Lee and Megan Willis) then uses a k-means clustering algorithm to compute an initial 10 clusters containing particles with similar spectra (Lee et al., 2019;Lee et al., 2015).

Temporal correlations and cosine similarity for different solutions of the single particle k-means clustering analysis were determined. The number of clusters for each solution was chosen using a threshold of 10% for the average fraction of total particles for each cluster. Tables S8-9 summarizes the 2 to 10 cluster solutions and criteria of single particle analysis. A 5-cluster solution was selected for Autumn and Early Spring marine periods, a 6-cluster solution was selected for the Autumn continental period, and a 7-cluster solution was selected for the Early Spring continental period.

Each cluster was categorized as oxidized organic aerosol (OOA), hydrocarbon-like organic aerosol (HOA), partially sulfate (PS), or mostly sulfate (MS) particle types. Clusters were considered organic (OOA, HOA) when 70% or more of the ion signal was organic (fORG > 70%). Organic clusters were further categorized as HOA when the highest ion signal was observed at m/z 43 ($C_3H_7^+$) and as OOA when highest ion signal was observed at m/z 44 (CO_2^+). The HOA cluster also required a larger fraction (>10%) of the ion signal from the sum of peaks in the alkane series $C_xH_{2y-1}^+$ and $C_xH_{2y+1}^+$, namely m/z 41 ($C_3H_5^+$), m/z 55 ($C_4H_7^+$), and m/z 57 ($C_4H_9^+$), than the OOA particle type (<10%). The peak at m/z 43 was not considered in this calculation since m/z 43 in OOA's mass spectrum is likely from $C_2H_3O^+$ rather than $C_3H_7^+$. Clusters were considered sulfate (PS, MS) when 40% or more of the ion signal was sulfate (fSO_4 > 40%). The MS particle type additionally required 65% of the ion signal to be sulfate ($fSO_4 \geq$ 65%). The mass spectra of PS particle type also met the criteria of attributing 30% or more of the ion signal to organics (fORG > 30%).

For each period, MS and PS clusters were further combined into a single MS cluster and a single PS cluster. One OOA cluster was resolved for all periods except during continental periods in Autumn when there were two OOA clusters (OOA-I, OOA-II). A single HOA cluster was resolved for continental air masses in Autumn. The mass spectra and time series of each particle type are found in Figures S8-12. The normalized UMR mass spectrum is used to find the signal from AMS NR single particle amine fragments by summing the product of the total ion signal fraction of each m/z in the spectrum and the average fraction of AMS NR single particle amine fragments attributed to the same m/z (estimated in Table S7). These results, along with a summary of the single particle measurements and particle types, are found in Table S10.

The mass spectra of the OOA particle type shows prominent peaks at m/z 29 (CHO^+), m/z 43 ($C_2H_3O^+$), and m/z 44 (CO_2^+). During continental Autumn periods, when two separate OOA clusters were resolved, the sum of these oxidized organic peaks was greater in the mass spectrum of OOA-II than that of OOA-I, indicating different magnitudes of particle aging. In

Early Spring, OOA particles contained larger contributions from sulfate fragments identified from peaks at m/z 48 (SO^+), m/z 64 ($SO2^+$), m/z 80 (SO_3^+), m/z 81 (HSO_3^+), m/z 96 (SO_4^+), and m/z 98 ($H_2SO_4^+$). These sulfate peaks were most prominent in the mass spectrum of the OOA particle type during the continental periods in Early Spring. Additionally, the OOA particle type was more abundant relative to other particle types within continental air masses in Autumn. OOA particles made up a greater fraction of the total particle count during continental periods than during marine periods. The signal attributed to AMS NR single particle amine fragments for the OOA particle type was greater when air masses were marine. Specifically, the AMS NR single particle amine fragment fraction of the OOA mass spectrum's ion signal was 3.6% and 3.2% for marine periods and 2.3-2.8% and 2.8% for continental periods during Autumn and Early Spring, respectively. The OOA particle type had the largest contributions from AMS NR single particle amine fragments among all particle types except during continental periods in Autumn.

The HOA particle type contained substantial contributions from m/z 29 (CHO^+), m/z 43 (C_3H_7), and m/z 44 (CO_2^+) as well as m/z 55 ($C_4H_7^+$) and m/z 57 ($C_4H_9^+$) within its mass spectrum. Unlike the OOA particle type, the peaks at m/z 43 and m/z 55 are larger than the peak at m/z 44. The highest contribution from AMS NR single particle amine fragments observed in continental air masses during Autumn was for the HOA particle type with AMS NR single particle amine fragments accounting for 2.9% of the total ion signal. However, the HOA particle type made up only 15.3% of the total particle count during this period.

The MS particle type contained large peaks at m/z 48 (SO^+), m/z 64 ($SO2^+$), m/z 80 (SO_3^+), m/z 81 (HSO_3^+), m/z 96 (SO_4^+), and m/z 98 ($H_2SO_4^+$) within its mass spectra. This particle type had the smallest contributions from AMS NR single particle amine fragments (1.0-1.4% of the ion signal) but was the most abundant across all air masses except for continental Autumn air masses. The mass spectrum of the PS particle type contained both sulfate (m/z 48, m/z 64, m/z 80, m/z 81, and m/z 96) and organic (m/z 29, m/z 43, m/z 44) contributions. In Early Spring, the oxidized organic peaks were less significant in the MS mass spectra than in Autumn. The signal apportioned to AMS NR single particle amine fragments for the PS particle type ranged from 1.1-1.9% of the total ion signal.

Correlations of particle types with various tracers are shown in Tables S11-14. The organic (OOA & HOA) particle types had a moderate to strong correlation ($0.50 < R < 0.80$) to the LVOOA factor that was resolved in Autumn. Similarly, the sulfate (PS & MS) particle types had a weak to strong correlation ($0.68 < R < 0.86$) to the Sulfate factor for both air masses and seasons. This correlation was weakest for marine air masses in Early Spring and strongest for marine air masses in Autumn. No particle type had correlated with the Amine factor during any period.

Non-refractory AMS species used to identify sources of single particle clusters included AMS NR OM, AMS NR nitrate, AMS NR sulfate, AMS NR ammonium, and AMS NR chloride. Moderate correlations ($0.57 < R < 0.75$) of organic particle types and AMS NR OM were observed during Autumn. However, no correlation was found during Early Spring. The PS cluster resolved for marine air masses in Autumn is the only other particle type to correlate weakly ($R = 0.38$) to AMS NR OM during both seasons. Weak to moderate correlations ($0.38 <$

R < 0.69) of the organic particle types to AMS NR nitrate were observed for all periods except during continental periods in Early Spring. The strongest correlation with AMS NR nitrate was with the HOA particle type, suggesting an anthropogenic source. A weak correlation was also observed for the MS particle type during continental periods in Early Spring. Weak to strong correlations (0.28 < R < 0.85) of the sulfate particle types to AMS NR sulfate were observed during both seasons and periods. This correlation was weakest during marine periods in Early Spring and strongest during continental periods in Autumn. Weak to moderate correlations (0.32 < R < 0.64) of all particle types and AMS NR ammonium were observed throughout different seasons and were largely inconsistent. No particle type had correlated with AMS NR chloride.

IC inorganic ions included SO_4^{2-}, NO_3^-, NH_4^+, Na^+, MSA, Mg^{2+} K^+, Cl^-, Ca^{2+}, Br^-. Correlations with IC inorganic ions were insignificant for OOA particle types during marine periods in Early Spring and for MS particle types during continental periods in Autumn. Limited marine air mass sampling resulted in too few marine IC filters to retrieve correlation coefficients for marine air masses in Early Spring. Sulfate particle types had moderate to strong correlations with IC SO_4^{2-} (0.54 < R < 0.88) and IC NH_4^+ (0.50 < R < 0.95), and weak to strong correlations (0.30 < R < 0.94) with IC MSA when IC measurements were available. Weak to strong (0.27 < R < 0.84) correlations of IC NO_3^- and organic particle types were seen in Autumn. No correlations of any particle types with IC Br^- were observed.

Additional source associated tracers included atmospheric and seawater DMS, chlorophyll *a*, ozone, and radon. No positive correlations were observed for atmospheric DMS and any of the identified particle types. Positive correlations (R = 0.38-0.41) of seawater DMS and sulfate particle types were seen for marine air masses in Early Spring. Negative correlations (-0.34 < R < -0.25) of chlorophyll *a* and the PS particle type during Autumn and the OOA-II and MS particle types in continental air masses during Autumn were observed. The only positive correlation of chlorophyll *a* and a particle type was seen for the HOA particle type (R = 0.29). No particle type had correlated with chlorophyll *a* during Early Spring. A weak, positive correlation was observed for ozone and the OOA-I particle type during continental periods in Autumn and the OOA particle type in marine air masses during Early Spring. Alternatively, sulfate particle types in marine air masses in Autumn and continental air masses in Early Spring were shown to negatively correlate (-0.54 < R < -0.45) to ozone. Weak to moderate correlations (0.32 < R < 0.68) of radon and organic particle types during continental periods in Autumn and all particle types during marine periods in Early Spring were observed. However, the sulfate particle types had a negative correlation (-0.37 < R < -0.27) with radon within marine air masses in Autumn and continental air masses in Early Spring, indicating a local marine source.

Correlations of sea surface temperature (SST) did not display a consistent trend among particle types. Weak, positive correlations of photosynthetic activated radiation (PAR) and the HOA particle type (R = 0.35) and all particle types during marine periods in Early Spring (0.29 < R < 0.39) were found. Positive correlations (0.31 < R < 0.49) of sulfate particle types and relative humidity (RH) could indicate secondary organic aerosol formation in all periods except during marine periods in Early Spring. A weak, positive correlation (0.26 < R < 0.29) of wind speed and the sulfate particle types during continental Early Spring periods suggests a primary marine origin. Conversely, negative correlations are seen with the PS particle type during marine Early Spring periods, and the MS particle type during marine Autumn periods. No particle types

had correlated with CCN number concentration but the PS particle type during marine periods in Autumn weakly correlated to CCN/CN (R = 0.25). No positive correlations with atmospheric temperature were observed. Only weak, negative correlations (-0.38 < R < -0.27) were seen for the OOA-I and PS particle types during continental periods in Autumn and for the OOA particle type during marine periods in Early Spring.

S4. Linear Regressions and p-values for AMS NR Amine Fragments and FTIR NV Amine Groups

Pearson correlation (R) coefficients retrieved for AMS NR amine fragments and FTIR NV amine groups during all four seasons and both air mass types are available in Table 2 and 3, respectively. The corresponding p-values for correlation coefficients pertaining to AMS NR amine fragments are shown in Table S15. Table S16 contains the p-values of correlations with FTIR NV amine groups. Correlations with black carbon and IC inorganic ions ($nssK^+$ and MSA) were typically statistically insignificant for both AMS NR amine fragments and FTIR NV amine groups. For FTIR NV amine groups, correlations with AMS NR chloride and AMS NR nitrate were also mostly insignificant. Linear regressions for AMS NR amine fragments and numerous tracers are displayed in Table S17. Table S18 contains the linear regressions for FTIR NV amine groups.

S5. CCN Activity

The extent to which amine affects CCN activity is explored by determining particle hygroscopicity using SMPS and CCNC measurements made during the Autumn and Early Spring seasons. A thermodenuder Scanning Mobility Particle Sizer (SMPS) system was used to measure the number of particles with geometric mean diameters between ~0.02 and 0.5 μm. Unheated samples produced measurements with a time resolution of 2 minutes (Quinn et al., 2019). Measurements from the SMPS system and a Cloud Condensation Nuclei Counter (CCNC, DMT, Boulder, CO) measuring ambient CCN concentrations at 0.1% supersaturation were used to determine aerosol hygroscopicity. CCN measurements were taken every 10 seconds. Data from these two instruments were synchronized into 2-minute averaged data for further analysis.

The critical diameter is found by summing the number of particles from the bin with the largest diameter down to the bin with the diameter by which the following equation is satisfied:

1. $\frac{N_{CCN}}{N_{CN}} = 1$.

Hygroscopicity parameters (κ) are determined using SMPS and CCN counter data by the following equations:

2. $\kappa = \frac{4A^3}{27\, D_{crit}^3 \ln^2 Sc}$
3. $A = \frac{\sigma_{s/a}\, M_w}{RT\rho_w}$

where $\sigma_{s/a}$ is the surface tension of pure water (0.073 J m^{-2}), Sc is the ratio of supersaturation (for SS = 0.1%, $Sc = 1.01$), M_w is the molecular weight of water (18.016 g mol^{-1}), ρ_w is the density of water (1000 kg mol^{-1}), R is the universal gas constant (8.3145 J mol^{-1} K^{-1}), T is the ambient temperature (298.15 K) , and D_{crit} is the diameter by which 100% of particles have activated to CCN (Petters and Kreidenweis, 2007).

Measurements when CCN/CN >1 and when the CCN count was less than 100 cm^{-3} were excluded from the dataset. Table S19 contains a summary of the remaining measurements. The low duty cycle of ambient sampling coupled with low CCN concentrations resulted in only a finite number of κ estimates that limited further interpretation.

S6. Tracer and Amine Sources

Figure S13 displays the sources of tracers and amine in marine environments. Continental sources of gaseous amine and tracers such as $nssK^+$, black carbon, AMS NR nitrate, ozone, carboxylic acid, and radon include combustion (vehicular, industrial), agriculture, and biomass burning. Marine sources of amine in primary and secondary aerosols and tracers such as AMS NR chloride, IC sea salt, chlorophyll *a*, FTIR NV alcohol groups, IC MSA, as well as atmospheric and seawater DMS are linked to biological (microbial decomposition) and mechanical (wave breaking, bubble bursting) processes.

Table S1. Summary of solutions and criteria used for PMF analysis of AMS NR HR-Org and AMS NR HR-SO_4 for marine air masses in Autumn. Criteria that are not applicable for one factor are indicated by N/A. Paired clusters that do not have uncentered correlation coefficients (UC) higher than 0.8 are indicated by None.

Criteria \ Factor number (p)		1	2	3	4	5	6	7
Diff	Q/Q_{exp}	1.00	0.79	0.73	0.71	0.69	0.66	0.65
	Absolute residual	40.0	19.8	19.2	14.3	12.1	12.6	13.3
	Temporal correlation factors strength (R > 0.8)	N/A	None	None	None	None	None	None
	Similarity of factor spectra (R > 0.8)	N/A	None	None	2 pairs	3 pairs	2 pairs	5 pairs
	Factors with less than 10% total mass	None	None	1 factor	1 factor	2 factors	3 factors	5 factors
OminusC	Q/Q_{exp}	2.39	2.15	2.12	2.11	2.11	2.09	2.09
	Absolute residual	46.0	28.0	33.6	32.8	29.5	28.6	28.0
	Temporal correlation factors strength (R >0.8)	N/A	None	None	None	None	1 pair	3 pairs
	Similarity of factor spectra (R > 0.8)	N/A	None	1 pair	1 pair	3 pairs	3 pairs	2 pairs
	Factors with less than 10% total mass	None	None	None	1 factor	1 factor	2 factors	2 factors

Table S2**.** Summary of solutions and criteria used for PMF analysis of AMS NR HR-Org and AMS NR HR-SO_4 for continental air masses in Autumn. Criteria that are not applicable for one factor are indicated by N/A. Paired clusters that do not have uncentered correlation coefficients (UC) higher than 0.8 are indicated by None.

Criteria \ Factor number (p)		1	2	3	4	5	6	7
Diff	Q/Q_{exp}	2.74	2.14	2.05	1.93	1.88	1.82	1.79
	Absolute residual	30.8	16.9	14.5	12.7	8.92	10.3	8.67
	Temporal correlation factors strength (R > 0.8)	N/A	None	None	None	None	None	None
	Similarity of factor spectra (R > 0.8)	N/A	None	1 pair	1 pair	2 pairs	6 pairs	5 pairs
	Factors with less than 10% total mass	None	None	None	1 factor	1 factor	3 factors	3 factors
OminusC	Q/Q_{exp}	3.37	2.82	2.71	2.58	2.55	2.53	2.51
	Absolute residual	81.9	97.9	70.6	71.4	69.8	63.9	64.0
	Temporal correlation factors strength (R >0.8)	N/A	None	None	None	None	2 pairs	1 pair
	Similarity of factor spectra (R > 0.8)	N/A	None	None	1 pair	1 pair	1 pair	3 pairs
	Factors with less than 10% total mass	None	None	1 factor	2 factors	3 factors	4 factors	5 factors

Table S3. Summary of solutions and criteria used for PMF analysis of AMS NR HR-Org and AMS NR HR-SO_4 for marine air masses in Early Spring. Criteria that are not applicable for one factor are indicated by N/A. Paired clusters that do not have uncentered correlation coefficients (UC) higher than 0.8 are indicated by None.

Criteria \ Factor number (p)		1	2	3	4	5	6	7
Diff	Q/Q_{exp}	0.55	0.51	0.48	0.48	0.45	0.43	0.41
	Absolute residual	30.2	28.4	23.3	22.7	20.9	19.5	19.4
	Temporal correlation factors strength (R > 0.8)	N/A	None	None	None	None	None	None
	Similarity of factor spectra (R > 0.8)	N/A	None	1 pair	3 pairs	None	None	15 pairs
	Factors with less than 10% total mass	None	1 factor	1 factor	2 factors	2 factors	3 factors	4 factors
OminusC	Q/Q_{exp}	0.88	0.88	0.87	0.86	0.86	0.85	0.85
	Absolute residual	34.6	28.7	29.0	31.3	31.0	31.8	32.3
	Temporal correlation factors strength (R >0.8)	N/A	None	None	1 pair	None	None	None
	Similarity of factor spectra (R > 0.8)	N/A	None	1 pair	1 pair	1 pair	1 pair	2 pairs
	Factors with less than 10% total mass	None	None	None	None	1 factor	2 factors	2 factors

Table S4. Summary of solutions and criteria used for PMF analysis of AMS NR HR-Org and AMS NR HR-SO_4 for continental air masses in Early Spring. Criteria that are not applicable for one factor are indicated by N/A. Paired clusters that do not have uncentered correlation coefficients (UC) higher than 0.8 are indicated by None.

Criteria \ Factor number (p)		1	2	3	4	5	6	7
Diff	Q/Q_{exp}	0.38	0.34	0.31	0.29	0.28	0.28	0.26
	Absolute residual	29.8	28.3	8.45	8.40	8.38	7.71	7.64
	Temporal correlation factors strength (R > 0.8)	N/A	None	None	None	None	None	None
	Similarity of factor spectra (R > 0.8)	N/A	None	1 pair	None	None	None	1 pair
	Factors with less than 10% total mass	None	1 factor	1 factor	2 factors	3 factors	3 factors	4 factors
OminusC	Q/Q_{exp}	0.88	0.88	0.87	0.86	0.86	0.85	0.85
	Absolute residual	30.3	11.8	9.55	10.4	10.4	10.5	10.8
	Temporal correlation factors strength (R >0.8)	N/A	None	None	None	None	None	None
	Similarity of factor spectra (R > 0.8)	N/A	None	1 pair	1 pair	1 pair	2 pairs	4 pairs
	Factors with less than 10% total mass	None	None	None	None	None	1 factor	2 factors

Table S5. Mean mass concentrations and standard deviations (ng m^{-3}) of each PMF factor resolved for marine and continental air masses in Autumn and Early Spring.

Factor / Air Mass/Season	LVOOA	Sulfate	Amine
Marine Autumn	184 ± 216	281 ± 224	17 ± 34
Marine Early Spring	--	493 ± 314	39 ± 70
Continental Autumn	995 ± 1602	590 ± 400	--
Continental Early Spring	--	609 ± 376	51 ± 90

Table S6. Mean mass concentrations and standard deviations (μg m^{-3}) of AMS NR single particle amine fragments for marine and continental air masses in Autumn and Early Spring.

		Autumn		Early Spring	
m/z	Ion Fragment	Marine	Continental	Marine	Continental
27	CHN^+	0.0017 ± 0.0006	0.0045 ± 0.0041	0.0022 ± 0.0011	0.0021 ± 0.0006
29	CH_3N^+	0.0002 ± 0.0004	0.0001 ± 0.0001	0.0004 ± 0.0004	0.0002 ± 0.0001
30	CH_4N^+	0.0015 ± 0.0004	0.0024 ± 0.0022	0.0011 ± 0.0005	0.0008 ± 0.0003
41	$C_2H_3N^+$	0.0011 ± 0.0005	0.0029 ± 0.0027	0.0010 ± 0.0004	0.0012 ± 0.0004
42	$C_2H_4N^+$	0.0008 ± 0.0006	0.0016 ± 0.0014	0.0010 ± 0.0003	0.0009 ± 0.0002
43	$CHNO^+$ $C_2H_5N^+$	0.0012 ± 0.0004 0.0007 ± 0.0004	0.0029 ± 0.0023 0.0011 ± 0.0008	0.0014 ± 0.0009 0.0008 ± 0.0002	0.0013 ± 0.0004 0.0008 ± 0.0002
44	$C_2H_6N^+$	0.0005 ± 0.0002	0.0012 ± 0.0011	0.0010 ± 0.0005	0.0003 ± 0.0011
58	$C_2H_4NO^+$ $C_3H_8N^+$	0.0005 ± 0.0001 0.0002 ± 0.0001	0.0007 ± 0.0003 0.0004 ± 0.0003	0.0006 ± 0.0003 0.0004 ± 0.0002	0.0004 ± 0.0001 0.0003 ± 0.0001
59	$C_2H_5NO^+$ $C_3H_9N^+$	0.0004 ± 0.0001 0.0001 ± 0.0001	0.0006 ± 0.0004 0.0001 ± 0.0001	0.0004 ± 0.0002 0.0001 ± 0.0002	0.0003 ± 0.0001 0.0001 ± 0.0001
63	C_4HN^+	0.0031 ± 0.0003	0.0030 ± 0.0005	0.0010 ± 0.0004	0.0013 ± 0.0003
72	$C_3H_6NO^+$ $C_4H_{10}N^+$	0.0002 ± 0.0001 0.0001 ± 0.0001	0.0004 ± 0.0002 0.0001 ± 0.0001	0.0005 ± 0.0006 0.0002 ± 0.0001	0.0002 ± 0.0001 0.0001 ± 0.0001
73	$C_2H_3NO_2^+$ $C_2H_5N_2O^+$ $C_3H_7NO^+$ $C_4H_{11}N^+$	0.0003 ± 0.0001 0.0022 ± 0.0008 0.0019 ± 0.0005 0.0002 ± 0.0001	0.0007 ± 0.0005 0.0024 ± 0.0009 0.0019 ± 0.0003 0.0002 ± 0.0001	0.0003 ± 0.0001 0.0021 ± 0.0009 0.0019 ± 0.0010 0.0002 ± 0.0001	0.0002 ± 0.0001 0.0016 ± 0.0006 0.0016 ± 0.0005 0.0001 ± 0.0001
84	$C_4H_6NO^+$ $C_5H_{10}N^+$	0.0001 ± 0.0001 0.0001 ± 0.0001	0.0003 ± 0.0003 0.0002 ± 0.0002	0.0001 ± 0.0001 0.0003 ± 0.0003	0.0002 ± 0.0001 0.0002 ± 0.0001
85	$C_4H_7NO^+$ $C_5H_{11}N^+$	0.0003 ± 0.0003 0.0002 ± 0.0001	0.0003 ± 0.0002 0.0003 ± 0.0005	0.0002 ± 0.0001 0.0003 ± 0.0001	0.0002 ± 0.0001 0.0003 ± 0.0001
86	$C_4H_8NO^+$ $C_5H_{12}N^+$	0.0001 ± 0.0001 0.0001 ± 0.0001	0.0001 ± 0.0001 0.0001 ± 0.0001	0.0001 ± 0.0001 0.0001 ± 0.0001	0.0001 ± 0.0001 0.0001 ± 0.0001
100	$C_4H_8N_2O^+$ $C_5H_{10}NO^+$ $C_6H_{14}N^+$	0.0001 ± 0.0001 0.0001 ± 0.0001 0.0001 ± 0.0001	0.0001 ± 0.0001 0.0001 ± 0.0001 0.0001 ± 0.0001	0.0001 ± 0.0001 0.0001 ± 0.0001 0.0001 ± 0.0001	0.0001 ± 0.0001 0.0001 ± 0.0001 0.0001 ± 0.0001
101	$C_6H_{15}N^+$	0.0001 ± 0.0001	0.0001 ± 0.0001	0.0001 ± 0.0001	0.0001 ± 0.0001
Total	----	0.0180 ± 0.0056	0.0288 ± 0.0174	0.0180 ± 0.0040	0.0155± 0.0018

Table S7. Mean ion signal fractions and standard deviations of AMS NR single particle amine fragments for marine and continental air masses in Autumn and Early Spring.

		Autumn		Early Spring	
m/z	Ion Fragment	Marine	Continental	Marine	Continental
27	CHN^+	0.211 ± 0.064	0.160 ± 0.064	0.318 ± 0.156	0.238 ± 0.062
29	CH_3N^+	0.001 ± 0.001[a]	0.001 ± 0.001	0.001 ± 0.001	0.001 ± 0.001
30	CH_4N^+	0.099 ± 0.088	0.074 ± 0.032	0.084 ± 0.042	0.039 ± 0.008
41	$C_2H_3N^+$	0.123 ± 0.033	0.097 ± 0.036	0.194 ± 0.076	0.196 ± 0.061
42	$C_2H_4N^+$	0.104 ± 0.049	0.076 ± 0.040	0.168 ± 0.047	0.112 ± 0.044
43	$CHNO^+$ $C_2H_5N^+$	0.090 ± 0.023 0.052 ± 0.020	0.062 ± 0.027 0.029 ± 0.017	0.139 ± 0.042 0.108 ± 0.028	0.106 ± 0.053 0.057 ± 0.021
44	$C_2H_6N^+$	0.004 ± 0.003	0.003 ± 0.001	0.008 ± 0.006	0.004 ± 0.001
58	$C_2H_4NO^+$ $C_3H_8N^+$	0.204 ± 0.042 0.110 ± 0.037	0.149 ± 0.057 0.072 ± 0.031	0.199 ± 0.041 0.136 ± 0.047	0.174 ± 0.037 0.107 ± 0.037
59	$C_2H_5NO^+$ $C_3H_9N^+$	0.126 ± 0.020 0.051 ± 0.018	0.112 ± 0.035 0.040 ± 0.018	0.118 ± 0.062 0.064 ± 0.030	0.109 ± 0.045 0.060 ± 0.019
63	C_4HN^+	0.405 ± 0.030	0.321 ± 0.097	0.217 ± 0.071	0.334 ± 0.067
72	$C_3H_6NO^+$ $C_4H_{10}N^+$	0.083 ± 0.020 0.040 ± 0.010	0.081 ± 0.019 0.034 ± 0.015	0.149 ± 0.129 0.078 ± 0.030	0.102 ± 0.038 0.062 ± 0.019
73	$C_2H_3NO_2^+$ $C_2H_5N_2O^+$ $C_3H_7NO^+$ $C_4H_{11}N^+$	0.050 ± 0.018 0.186 ± 0.042 0.160 ± 0.030 0.042 ± 0.022	0.066 ± 0.028 0.173 ± 0.051 0.141 ± 0.041 0.032 ± 0.017	0.171 ± 0.373 0.157 ± 0.049 0.152 ± 0.066 0.046 ± 0.029	0.050 ± 0.024 0.176 ± 0.063 0.164 ± 0.053 0.038 ± 0.013
84	$C_4H_6NO^+$ $C_5H_{10}N^+$	0.101 ± 0.022 0.096 ± 0.021	0.086 ± 0.025 0.080 ± 0.040	0.079 ± 0.033 0.132 ± 0.106	0.083 ± 0.023 0.116 ± 0.057
85	$C_4H_7NO^+$ $C_5H_{11}N^+$	0.146 ± 0.056 0.086 ±0.022	0.092 ± 0.050 0.059 ± 0.029	0.108 ± 0.043 0.118 ± 0.037	0.119 ± 0.045 0.099 ± 0.031
86	$C_4H_8NO^+$ $C_5H_{12}N^+$	0.105 ± 0.155 0.088 ± 0.033	0.061 ± 0.021 0.054 ± 0.026	0.108 ± 0.034 0.084 ± 0.029	0.111 ± 0.036 0.084 ± 0.024
100	$C_4H_8N_2O^+$ $C_5H_{10}NO^+$ $C_6H_{14}N^+$	0.075 ± 0.022 0.038 ± 0.016 0.061 ± 0.023	0.037 ± 0.019 0.034 ± 0.030 0.046 ± 0.027	0.032 ± 0.016 0.035 ± 0.023 0.082 ± 0.044	0.038 ± 0.015 0.034 ± 0.025 0.067 ± 0.063
101	$C_6H_{15}N^+$	0.066 ± 0.024	0.027 ± 0.021	0.092 ± 0.027	0.058 ± 0.026

Table S8. Summary of criteria used for cluster analysis of single particle ET measurements taken in Autumn. Paired clusters that do not have uncentered correlation coefficients (UC) higher than 0.8 are indicated by None.

Criteria \ Cluster number (p)		2	3	4	5	6	7	8	9	10
Marine	Temporal correlation clusters strength (R > 0.8)	None	1 pair	2 pairs	4 pairs	7 pairs	11 pairs	10 pairs	12 pairs	16 pairs
	Similarity of cluster spectra (R > 0.8)	None	1 pair	2 pairs	4 pairs	7 pairs	11 pairs	10 pairs	12 pairs	15 pairs
	Clusters with less than 10% total count	None	None	None	None	2 clusters	3 clusters	4 clusters	4 clusters	6 clusters
Continental	Temporal correlation clusters strength (R > 0.8)	None	1 pair	1 pair	3 pairs	5 pairs	8 pairs	9 pairs	10 pairs	15 pairs
	Similarity of cluster spectra (R > 0.8)	None	1 pair	2 pairs	3 pairs	5 pairs	9 pairs	9 pairs	10 pairs	15 pairs
	Clusters with less than 10% total count	None	None	None	None	None	4 clusters	5 clusters	5 clusters	7 clusters

Table S9. Summary of criteria used for cluster analysis of single particle ET measurements taken in Early Spring. Paired clusters that do not have uncentered correlation coefficients (UC) higher than 0.8 are indicated by None.

Criteria \ Cluster number (p)		2	3	4	5	6	7	8	9	10
Marine	Temporal correlation clusters strength (R > 0.8)	1 pair	2 pairs	4 pairs	4 pairs	8 pairs	7 pairs	12 pairs	14 pairs	20 pairs
	Similarity of cluster spectra (R > 0.8)	1 pair	2 pairs	4 pairs	4 pairs	8 pairs	7 pairs	12 pairs	14 pairs	20 pairs
	Clusters with less than 10% total count	None	None	None	None	1 cluster	1 cluster	2 clusters	8 clusters	9 clusters
Continental	Temporal correlation clusters strength (R > 0.8)	1 pair	3 pairs	3 pairs	4 pairs	7 pairs	9 pairs	16 pairs	18 pairs	20 pairs
	Similarity of cluster spectra (R > 0.8)	1 pair	3 pairs	3 pairs	4 pairs	8 pairs	9 pairs	16 pairs	18 pairs	21 pairs
	Clusters with less than 10% total count	None	None	None	None	None	None	1 cluster	3 clusters	3 clusters

Table S10. Summary of single particle measurements and aerosol types and identified by ET mode for marine and continental air masses in Autumn and Early Spring.

Statistic \ Particle Type		OOA	OOA-I	OOA-II	HOA	PS	MS
Marine Autumn	Particle count	15121	--	--	--	17849	19715
	Fraction of total particle count	28.7%	--	--	--	33.9%	37.4%
	Signal from AMS NR single particle amine fragments relative to the total ion signal	3.6%	--	--	--	1.9%	1.4%
	Signal from AMS NR single particle amine fragments relative to the total organic ion signal	4.6%	--	--	--	4.4%	7.5%
Marine Early Spring	Particle count	1098	--	--	--	1934	6489
	Fraction of total particle count	11.5%	--	--	--	20.3%	68.2%
	Signal from AMS NR single particle amine fragments relative to the total ion signal	3.2%	--	--	--	1.4%	1.3%
	Signal from AMS NR single particle amine fragments relative to the total organic ion signal	3.8%	--	--	--	3.7%	8.1%
Continental Autumn	Particle count	--	8522	5525	5448	10390	5709
	Fraction of total particle count	--	23.9%	15.5%	15.3%	29.2%	16.0%
	Signal from AMS NR single particle amine fragments relative to the total ion signal	--	2.8%	2.3%	2.9%	1.7%	1.1%
	Signal from AMS NR single particle amine fragments relative to the total organic ion signal	--	3.3%	2.7%	3.2%	3.8%	5.9%
Continental Early Spring	Particle count	8412	--	--	--	7851	40771
	Fraction of total particle count	14.7%	--	--	--	13.7%	71.5%
	Signal from AMS NR single particle amine fragments relative to the total ion signal	2.8%	--	--	--	1.1%	1.0%
	Signal from AMS NR single particle amine fragments relative to the total organic signal	3.9%	--	--	--	3.4%	7.1%

Table S11. Pearson correlation (R) coefficient values between ET single particle types and other measured properties for marine air masses in Autumn. Negative correlations are shaded blue and positive correlations are shaded red. The strength of each correlation determines the level of saturation for the corresponding shading- no correlation ($|R| < 0.25$)- gray, weak correlation ($0.25 \leq |R| < 0.50$)- light blue/red, moderate correlation ($0.50 \leq |R| < 0.80$)- medium blue/red, strong correlation ($0.80 \leq |R|$)- dark blue/red. All correlations shown are statistically significant ($p < 0.05$).

Particle Type / Tracer	OOA	PS	MS
LVOOA Factor	0.80	-0.09	-0.29
Sulfate Factor	-0.09	0.83	0.86
Amine Factor	-0.17	0.03	0.10
CCN/CN	-0.06	0.25	0.24
CCN Count	-0.18	0.08	0.04
atm. DMS	-0.10	0.38	0.32
sw. DMS	0.16	-0.14	-0.19
AMS NR OM	0.75	0.31	0.13
AMS NR Nitrate	0.38	0.16	0.05
AMS NR Sulfate	-0.07	0.83	0.85
AMS NR Ammonium	-0.04	0.37	0.45
AMS NR Chloride	-0.14	-0.09	-0.05
IC SO_4^{2-}	0.12	0.85	0.88
IC NO_3^-	0.84	0.22	0.22
IC NH_4^+	0.00	0.95	0.95
IC Na^+	0.63	-0.01	0.03
IC MSA	0.64	0.41	0.49
IC Mg^{2+}	0.65	-0.02	0.02
IC K^+	0.37	0.14	0.19
IC Cl^-	0.60	-0.12	-0.08
IC Ca^{2+}	0.67	-0.20	-0.16
IC Br^-	-0.18	-0.15	-0.24
IC Sea salt	0.62	-0.06	-0.02
Chlorophyll *a*	-0.23	-0.27	-0.17
Ozone	0.02	-0.47	-0.54
Radon	0.18	-0.37	-0.36
Sea Surface Temperature	-0.12	0.45	0.45
Photosynthetically Activated Radiation	0.13	-0.10	-0.11
Relative Humidity	-0.21	0.42	0.46
Wind Speed	0.09	-0.24	-0.37
Atmospheric Temperature	0.01	0.14	0.13

Table S12. Pearson correlation (R) coefficient values between ET single particle types and other measured properties for continental air masses in Autumn. Negative correlations are shaded blue and positive correlations are shaded red. The strength of each correlation determines the level of saturation for the corresponding shading- no correlation ($|R| < 0.25$)- gray, weak correlation ($0.25 \leq |R| < 0.50$)- light blue/red, moderate correlation ($0.50 \leq |R| < 0.80$)- medium blue/red, strong correlation ($0.80 \leq |R|$)- dark blue/red. Correlations that are not statistically significant ($p \geq 0.05$) are indicated by *. A two-tailed T test is used to estimate p-values.

Tracer \ Particle Type	OOA-I	OOA-II	HOA	PS	MS
LVOOA Factor	0.69	0.50	0.61	-0.33	-0.31
Sulfate Factor	-0.08	0.29	-0.16	0.69	0.68
CCN Measurements	--	--	--	--	--
atm. DMS	-0.07	-0.35	-0.06	-0.46	-0.22
sw. DMS	-0.03	-0.16	-0.03	-0.16	-0.08
AMS NR OM	0.68	0.57	0.64	-0.24	-0.23
AMS NR Nitrate	0.58	0.38	0.69	-0.26	-0.24
AMS NR Sulfate	0.17	0.46	0.07	0.56	0.57
AMS NR Ammonium	0.49	0.64	0.32	0.24	0.21
AMS NR Chloride	-0.07	-0.04	-0.03	-0.04	-0.01
IC SO_4^{2-}	-0.18	0.61	-0.20	0.81	0.81*
IC NO_3^-	0.14	0.27	0.66	0.11	0.10*
IC NH_4^+	-0.21	0.56	-0.31	0.83	0.83*
IC Na^+	0.17	-0.65	0.51	-0.71	-0.71*
IC MSA	-0.65	-0.27	0.11	0.30	0.30*
IC Mg^{2+}	0.35	-0.48	0.65	-0.81	-0.81*
IC K^+	0.97	0.62	0.60	-0.60	-0.61*
IC Cl^-	-0.18	-0.87	0.21	-0.57	-0.57*
IC Ca^{2+}	0.48	-0.20	0.87	-0.79	-0.80*
IC Br^-	--	--	--	--	--
IC Sea salt	0.01	-0.78	0.39	-0.68	-0.68
Chlorophyll *a*	0.13	-0.25	0.29	-0.32	-0.34
Ozone	0.24	0.44	-0.09	0.07	-0.01
Radon	0.49	0.44	0.36	0.11	-0.03
Sea Surface Temperature	0.27	0.34	0.11	-0.05	-0.05
Photosynthetically Activated Radiation	0.18	0.16	0.35	-0.22	-0.20
Relative Humidity	-0.25	-0.16	-0.16	0.49	0.46
Wind Speed	0.07	0.05	0.05	0.03	0.00
Atmospheric Temperature	-0.07	-0.27	-0.04	-0.29	-0.15

Table S13. Pearson correlation (R) coefficient values between ET single particle types and other measured properties for marine air masses in Early Spring. Negative correlations are shaded blue and positive correlations are shaded red. The strength of each correlation determines the level of saturation for the corresponding shading- no correlation ($|R| < 0.25$)- gray, weak correlation ($0.25 \leq |R| < 0.50$)- light blue/red, moderate correlation ($0.50 \leq |R| < 0.80$)- medium blue/red, strong correlation ($0.80 \leq |R|$)- dark blue/red. All correlations shown are statistically significant ($p < 0.05$). A two-tailed T test is used to estimate p-values.

Particle Type / Tracer	OOA	PS	MS
Sulfate Factor	-0.20	0.29	0.28
Amine Factor	0.18	-0.05	-0.01
CCN Measurements	--	--	--
atm. DMS	-0.26	0.03	-0.04
sw. DMS	-0.04	0.41	0.38
AMS NR OM	-0.03	-0.05	-0.05
AMS NR Nitrate	0.52	0.18	0.28
AMS NR Sulfate	-0.19	0.29	0.28
AMS NR Ammonium	-0.24	0.13	0.04
AMS NR Chloride	0.37	0.28	0.29
IC Measurements	--	--	--
Chlorophyll *a*	-0.09	-0.03	0.01
Ozone	0.30	0.03	0.08
Radon	0.68	0.25	0.48
Sea Surface Temperature	-0.50	-0.25	-0.31
Photosynthetically Activated Radiation	0.29	0.39	0.36
Relative Humidity	-0.14	0.19	0.17
Wind Speed	0.04	-0.26	-0.24
Atmospheric Temperature	-0.38	-0.14	-0.19

Table S14. Pearson correlation (R) coefficient values between ET single particle types and other measured properties for continental air masses in Early Spring. Negative correlations are shaded blue and positive correlations are shaded red. The strength of each correlation determines the level of saturation for the corresponding shading- no correlation ($|R| < 0.25$)- gray, weak correlation ($0.25 \leq |R| < 0.50$)- light blue/red, moderate correlation ($0.50 \leq |R| < 0.80$)- medium blue/red, strong correlation ($0.80 \leq |R|$)- dark blue/red. Correlations that are not statistically significant ($p \geq 0.05$) are indicated by *. A two-tailed T test is used to estimate p-values.

Particle Type / Tracer	OOA	PS	MS
Sulfate Factor	0.14	0.69	0.79
Amine Factor	-0.05	-0.23	-0.17
CCN/CN	0.02	0.17	0.17
CCN Count	-0.07	0.09	0.10
atm. DMS	-0.42	-0.10	-0.16
sw. DMS	-0.25	-0.38	-0.35
AMS NR OM	0.16	-0.10	0.08
AMS NR Nitrate	0.07	-0.28	-0.19
AMS NR Sulfate	0.14	0.70	0.80
AMS NR Ammonium	0.18	0.15	0.38
AMS NR Chloride	-0.11	0.21	0.13
IC SO_4^{2-}	-0.31*	0.54	0.58
IC NO_3^-	-0.28*	-0.52	-0.48
IC NH_4^+	-0.30*	0.50	0.55
IC Na^+	-0.28*	0.26	0.25
IC MSA	0.34*	0.89	0.94
IC Mg^{2+}	-0.29*	0.33	0.32
IC K^+	-0.30*	0.52	0.55
IC Cl^-	-0.20*	0.12	0.09
IC Ca^{2+}	-0.40*	0.41	0.43
IC Br^-	--	--	--
IC Sea salt	-0.24	0.20	0.18
Chlorophyll *a*	-0.02	-0.01	-0.04
Ozone	0.20	-0.45	-0.23
Radon	0.02	-0.27	-0.27
Sea Surface Temperature	0.11	-0.36	-0.12
Photosynthetically Activated Radiation	0.02	0.10	0.16
Relative Humidity	-0.08	0.40	0.31
Wind Speed	0.04	0.29	0.26
Atmospheric Temperature	0.01	0.12	0.14

Table S15. p-values retrieved for correlations of AMS NR amine fragments and various tracers for marine periods (columns 1-4) and continental periods (columns 5-8). p-values that are greater than 0.05 are statistically insignificant and are shaded in red. p-values that are less than 0.05 are statistically significant and are shaded in green. A two-tailed T test is used to estimate p-values.

Air Masses	Marine				Continental			
Season	Winter	Early Spring	Late Spring	Autumn	Winter	Early Spring	Late Spring	Autumn
AMS NR OM	0.00	0.00	0.00	0.00	0.00	0.00	0.00	0.00
FTIR NV OM	0.00	0.25	0.02	0.04	0.00	0.14	0.08	0.40
AMS NR Nitrate	0.00	0.00	0.00	0.00	0.00	0.00	0.27	0.00
AMS NR Sulfate	0.00	0.00	0.00	0.00	0.00	0.00	0.00	0.00
AMS NR Chloride	0.00	0.00	0.00	0.00	0.00	0.00	0.00	0.00
AMS NR m/z 44	0.00	0.00	0.00	0.00	0.00	0.00	0.00	0.00
Black Carbon	0.06	0.45	0.16	0.00	0.00	0.00	0.00	0.00
Ozone	0.00	0.00	0.00	0.00	0.00	0.00	0.00	0.00
Radon	0.00	0.00	0.00	0.00	0.00	0.00	0.00	0.00
Wind Speed	0.00	0.00	0.00	0.00	0.00	0.00	0.00	0.00
sw. DMS	0.00	0.00	0.01	0.00	0.00	0.00	0.00	0.00
atm. DMS	0.00	0.00	0.01	0.00	0.00	0.00	0.00	0.00
Solar Radiation	0.00	0.00	0.00	0.00	0.00	0.00	0.00	0.00
Relative Humidity	0.00	0.00	0.00	0.00	0.00	0.00	0.00	0.00
Temperature	0.00	0.00	0.00	0.00	0.00	0.00	0.00	0.00
Chlorophyll *a*	0.00	0.00	0.00	0.00	0.00	0.00	0.00	0.00
SST	0.00	0.00	0.00	0.00	0.00	0.00	0.00	0.00
IC MSA	--	--	0.24	0.00	--	0.20	0.54	0.00
IC Sea Salt	0.00	--	0.05	0.00	0.03	0.00	0.61	0.17
IC nssK^+	0.05	--	0.00	0.00	0.65	0.02	0.02	0.01

Table S16. p-values retrieved for correlations of FTIR NV amine groups (ADL & BDL) in particles with diameters <1 μm and various tracers for marine periods (columns 1-4) and continental periods (columns 5-8). p-values that are greater than 0.05 are statistically insignificant and are shaded in red. p-values that are less than 0.05 are statistically significant and are shaded in green. A two-tailed T test is used to estimate p-values.

Air Masses	Marine				Continental			
Season	Winter	Early Spring	Late Spring	Autumn	Winter	Early Spring	Late Spring	Autumn
AMS NR OM	0.00	--	0.00	0.00	0.00	0.00	0.03	--
FTIR NV OM	0.00	--	0.01	0.02	0.00	0.12	0.07	--
AMS NR Nitrate	0.33	--	0.30	0.98	0.18	0.93	0.32	--
AMS NR Sulfate	0.00	--	0.00	0.00	0.00	0.00	0.01	--
AMS NR Chloride	0.76	--	0.77	0.72	0.02	0.66	0.21	--
AMS NR m/z 44	0.00	--	0.00	0.00	0.00	0.00	0.00	--
Black Carbon	0.17	--	0.18	0.10	0.01	0.00	0.06	--
Ozone	0.00	--	0.00	0.00	0.00	0.00	0.00	--
Radon	0.00	--	0.00	0.00	0.00	0.00	0.00	--
Wind Speed	0.00	--	0.00	0.00	0.00	0.00	0.00	--
sw. DMS	0.00	--	0.01	0.00	0.00	0.00	--	--
atm. DMS	0.00	--	0.01	0.00	0.00	0.00	--	--
Solar Radiation	0.00	--	0.00	0.00	0.07	0.00	0.04	--
Relative Humidity	0.00	--	0.00	0.00	0.00	0.00	0.00	--
Temperature	0.00	--	0.00	0.00	0.00	0.00	0.00	--
Chlorophyll *a*	0.00	--	0.01	0.01	0.02	0.00	0.00	--
SST	0.00	--	0.00	0.00	0.00	0.00	0.00	--
IC MSA	--	--	0.09	0.36	--	0.36	0.15	--
IC Sea Salt	0.00	--	0.03	0.00	--	0.00	0.02	--
IC nssK^+	0.42	--	0.07	0.65	--	0.76	0.50	--

Table S17. Linear regressions (Y = mX + b) for various tracers versus AMS NR amine fragments for marine periods (columns 1-4) and continental periods (columns 5-8).

Air Masses	Marine				Continental			
Season	Winter	Early Spring	Late Spring	Autumn	Winter	Early Spring	Late Spring	Autumn
AMS NR OM	14X	4.8X + 0.1	28X	13X	31X	17X	34X	24X
FTIR NV OM	-21X	--	-2.4X + 0.3	19X	-17X + 1	39X -1	13X	--
AMS NR Nitrate	0.52X	-0.12X + 0.01	0.58X	0.08X + 0.01	1.1X	0.04X + 0.01	4.3X - 0.1	0.24X
AMS NR Sulfate	18X	26X	8.7X	5.0X + 0.1	22X	4.0X + 0.3	4.8X + 0.1	1.5X + 0.3
AMS NR Chloride	0.17X + 0.01	-0.04X + 0.01	-0.12X + 0.02	-0.04 + 0.01	0.16X + 0.01	-0.09X + 0.01	-0.08X + 0.02	-0.01X + 0.01
AMS NR m/z 44	3.5X	1.0X + 0.01	3.9X	2.2X + 0.1	6.5X	4.0X + 0.1	5.9X	4.6X + 0.1
Black Carbon	2.8X	-0.31X + 0.04	1.3X - 0.01	0.59X	12X	9.0X - 0.1	4.8X	3.7X
Ozone	91X + 40	-1568X + 84	-241X + 44	-142X + 33	-172X + 41	30X + 46	145X + 34	94X + 28
Radon	13811X + 60	-315X + 386	-1860X + 341	580X + 397	31344X + 34	7090X	10264X + 34	9747X
Wind Speed	-247X	-47X	-359X	14X	-0.43X	-174X	-28X	-28X
sw. DMS	15X + 1	-12X + 3	-34X + 4	3.7X + 3.2	7.1X + 1.3	27X + 4	-48X + 4	-7X + 3
atm. DMS	-1326X + 85	5945X -61	-6285X + 570	995X + 111	5049X + 14	-4689X + 226	-2971X + 331	2800X + 38
Solar Radiation	-891X + 65	163X + 3	3677X + 4	1656X + 3	-257X +1	7562X + 4	-902X + 4	1414X + 3
Relative Humidity	-2074X + 103	-2.5X + 78	-89X + 86	-46X + 83	174X + 74	-336X +79	28X + 77	-126X + 89
Temperature	-592X +18	572X + 2	-96X + 11	132X + 10	183X +9	132X +9	100X + 5	37X + 15
Chlorophyll *a*	-7.5X + 0.6	4.5X + 0.5	19X + 1	-12X + 1	16X	-3.9X + 0.7	-0.5X + 1.6	-2.0X + 0.4
SST	-265X + 17	465X + 6	-153X + 14	102X + 12	181X + 11	139X + 12	83X + 7	52X + 15
IC MSA	--	--	4.9X – 0.1	1.8X	--	13X	0.16X + 0.06	0X
IC Sea Salt	210X – 2	--	-44X + 1	60X – 1	-447X	20X + 1	-0.40X + 0.08	-0.47X + 0.48
IC nssK^+	3.3X	--	0.10X	0.33X	5.3X – 0.1	2.5X – 0.1	0.41X	0.35X -0.01

Table S18. Linear regressions (Y = mX + b) for various tracers versus FTIR NV amine groups (ADL & BDL) in particles with diameters <1 μm for marine periods (columns 1-4) and continental periods (columns 5-8).

Air Masses	Marine				Continental			
Season	Winter	Early Spring	Late Spring	Autumn	Winter	Early Spring	Late Spring	Autumn
AMS NR OM	-0.36X + 0.20	--	2.0X + 0.4	-1.7X + 0.3	1.6X + 0.5	2.2X + 0.4	33X + 2	--
FTIR NV OM	8.9X + 0.2	--	10X	10X	4.6X + 0.2	11.4X	2.1X + 0.4	--
AMS NR Nitrate	-0.02X	--	0.04X	-0.04X	0X	-0.02X	-3.0X + 0.1	--
AMS NR Sulfate	-0.93X + 0.01	--	3.2X + 0.2	3.7X + 0.2	2.6X + 0.3	-3.0X + 0.5	-4.9X + 0.4	--
AMS NR Chloride	0.12X	--	0.70X	0X	0.10X	0.13X	-0.05X	--
AMS NR m/z 44	-0.10X + 0.06	--	-0.82X + 0.15	-0.66X + 0.15	0.18X + 0.11	0.76X + 0.18	-5.1X + 0.4	--
Black Carbon	-32X + 1	--	-1.1X + 0.1	0.18X + 0.02	2.5X + 0.04	0.15X + 0.19	-1.3X + 0.1	--
Ozone	41X + 41	--	57X + 37	-94X + 28	19X +33	47X + 48	71X + 40	--
Radon	-3698X + 304	--	993X + 277	-1904X + 446	-4413X + 855	-67X + 886	-3048X + 616	--
Wind Speed	-62X + 11	--	-37X + 10	14X + 10	54X + 12	70X + 10.6	1.1X + 6.1	--
sw. DMS	-6.0X + 1.2	--	97X + 0.62	-46X + 3	7.6X + 0.2	-5.6X + 1.5	--	--
atm. DMS	-405X + 79	--	21137X + 135	-1216X + 80	1532X + 47	-235X + 64	--	--
Solar Radiation	-1848X + 73	--	621X + 147	-2647X + 149	1745X + 1	105X + 181	-13163X + 642	--
Relative Humidity	-145X + 75	--	314X + 79	-12X + 82	-114X + 1	-104X + 69	-156X + 642	--
Temperature	-98X + 11	--	-216X + 12	103X + 13	16X + 9	-5.6X + 12	-21X + 10	--
Chlorophyll *a*	1.7X + 0.4	--	61X	-5.2X + 0.3	-15X + 2	0.45X + 0.50	-7.9X + 1.4	--
SST	-110X + 14	--	-252X + 14	143X + 14	-46X +16	13X + 15	2.9X + 10.7	--
IC MSA	--	--	4X	-0.13X	--	-0.95X + 0.07	-1.1X + 0.1	--
IC Sea Salt	10X + 1	--	8.4X + 0.3	14X	--	9.2X + 0.9	-0.60X + 0.10	--
IC $nssK^+$	0.08X	--	0X + 0.06	0.003X + 0.009	--	0.13X + 0.01	-0.09X + 0.01	--

Table S19. Critical Diameters and Hygroscopicity Estimates, Continued

Time	Cruise	Air Mass	CCN (cm^{-3})	CN (cm^{-3})	CCN/CN	D_{crit} (μm)	κ
09/09/2017 04:08	3	M	104	282	0.37	0.14	0.57
09/09/2017 04:16	3	M	109	289	0.38	0.13	0.63
09/09/2017 04:18	3	M	110	289	0.38	0.13	0.70
09/15/2017 01:58	3	C	171	342	0.50	0.11	1.21
09/15/2017 06:28	3	C	140	295	0.48	0.10	1.34
09/15/2017 06:34	3	C	132	291	0.45	0.04	22.14
09/15/2017 06:36	3	C	138	290	0.47	0.11	1.21
09/15/2017 06:38	3	C	135	291	0.46	0.11	1.21
03/23/2018 11:24	4	M	109	206	0.53	0.02	112.04
03/23/2018 11:26	4	M	109	204	0.54	0.12	0.78
03/23/2018 11:28	4	M	109	205	0.53	0.11	1.08
03/23/2018 11:34	4	M	108	203	0.53	0.03	42.45
03/23/2018 11:36	4	M	107	204	0.52	0.11	0.97
03/23/2018 11:38	4	M	111	204	0.54	0.10	1.34
04/01/2018 17:44	4	C	150	506	0.30	0.07	3.54
04/01/2018 17:46	4	C	188	507	0.37	0.10	1.50
04/01/2018 17:48	4	C	199	515	0.39	0.10	1.34
04/01/2018 22:14	4	C	157	478	0.33	0.07	3.96
04/01/2018 22:16	4	C	180	480	0.37	0.11	1.08
04/01/2018 22:18	4	C	209	474	0.44	0.10	1.50
04/01/2018 22:24	4	C	205	477	0.43	0.05	9.36
04/01/2018 22:26	4	C	195	480	0.41	0.10	1.50
04/01/2018 22:28	4	C	173	500	0.35	0.11	1.08
04/02/2018 02:54	4	C	167	567	0.29	0.07	3.54
04/02/2018 02:56	4	C	195	562	0.35	0.11	1.21
04/02/2018 02:58	4	C	191	544	0.35	0.11	1.21
04/02/2018 03:04	4	C	181	532	0.34	0.06	6.76
04/02/2018 03:06	4	C	185	534	0.35	0.11	1.21
04/02/2018 03:08	4	C	178	532	0.34	0.11	1.08
04/03/2018 00:08	4	C	180	585	0.31	0.07	3.96
04/03/2018 04:34	4	C	159	506	0.31	0.05	10.44
04/03/2018 04:36	4	C	158	505	0.31	0.12	0.78
04/03/2018 04:38	4	C	158	502	0.31	0.12	0.78
04/03/2018 04:44	4	C	152	502	0.30	0.05	11.61
04/03/2018 04:46	4	C	154	501	0.31	0.12	0.87
04/03/2018 04:48	4	C	150	498	0.30	0.13	0.70
04/03/2018 09:18	4	C	101	427	0.24	0.13	0.70
04/03/2018 09:28	4	C	100	458	0.22	0.13	0.70
04/05/2018 03:24	4	C	105	201	0.52	0.10	1.34
04/05/2018 03:26	4	C	102	199	0.51	0.12	0.87
04/05/2018 03:28	4	C	101	202	0.50	0.10	1.50
04/07/2018 02:38	4	C	158	333	0.47	0.12	0.87
04/07/2018 02:44	4	C	165	336	0.49	0.11	1.08
04/07/2018 02:46	4	C	161	339	0.48	0.11	0.97
04/07/2018 02:48	4	C	163	340	0.48	0.11	1.08
04/07/2018 22:48	4	C	161	449	0.36	0.14	0.51
04/08/2018 03:18	4	C	208	423	0.49	0.11	0.97
04/08/2018 03:24	4	C	177	425	0.42	0.06	7.53
04/08/2018 03:26	4	C	221	425	0.52	0.11	1.21

04/08/2018 03:28	4	C	221	426	0.52	0.11	1.21
04/08/2018 07:58	4	C	156	285	0.55	0.09	2.07
04/08/2018 08:04	4	C	144	279	0.52	0.03	42.45
04/08/2018 08:06	4	C	150	279	0.54	0.10	1.50
04/08/2018 08:08	4	C	152	278	0.55	0.09	2.07
04/08/2018 12:36	4	C	114	282	0.41	0.11	1.21
04/08/2018 12:38	4	C	114	282	0.40	0.10	1.50
04/08/2018 12:44	4	C	111	282	0.39	0.03	38.04
04/08/2018 12:46	4	C	114	280	0.41	0.09	1.67
04/08/2018 12:48	4	C	115	281	0.41	0.10	1.50
04/09/2018 04:06	4	C	236	499	0.47	0.09	1.86
04/09/2018 04:08	4	C	241	502	0.48	0.09	1.86
04/09/2018 04:14	4	C	235	503	0.47	0.02	213.29
04/09/2018 04:16	4	C	255	517	0.49	0.09	2.30
04/09/2018 04:18	4	C	247	501	0.49	0.09	1.67
04/09/2018 16:34	4	C	203	687	0.29	0.11	1.08
04/09/2018 16:36	4	C	192	666	0.29	0.12	0.87
04/09/2018 16:38	4	C	192	666	0.29	0.05	14.47
04/10/2018 01:44	4	C	137	748	0.18	0.03	34.21
04/10/2018 01:46	4	C	157	744	0.21	0.08	2.57
04/10/2018 01:48	4	C	158	767	0.21	0.09	1.67
04/10/2018 01:54	4	C	163	752	0.22	0.02	101.25
04/10/2018 01:56	4	C	144	720	0.20	0.10	1.34
04/10/2018 01:58	4	C	137	697	0.20	0.10	1.50
04/10/2018 06:24	4	C	157	673	0.23	0.02	191.13
04/10/2018 06:26	4	C	136	678	0.20	0.11	1.21
04/10/2018 06:28	4	C	135	663	0.20	0.11	1.08
04/10/2018 06:34	4	C	156	696	0.22	0.02	112.04
04/10/2018 06:36	4	C	169	699	0.24	0.10	1.50
04/10/2018 06:38	4	C	156	714	0.22	0.11	1.21
04/10/2018 11:04	4	C	211	840	0.25	0.03	38.04
04/10/2018 11:06	4	C	215	841	0.26	0.11	1.08
04/10/2018 11:08	4	C	228	839	0.27	0.10	1.34
04/10/2018 11:14	4	C	250	885	0.28	0.02	191.13
04/10/2018 11:16	4	C	200	872	0.23	0.12	0.87
04/10/2018 11:18	4	C	217	863	0.25	0.11	1.21

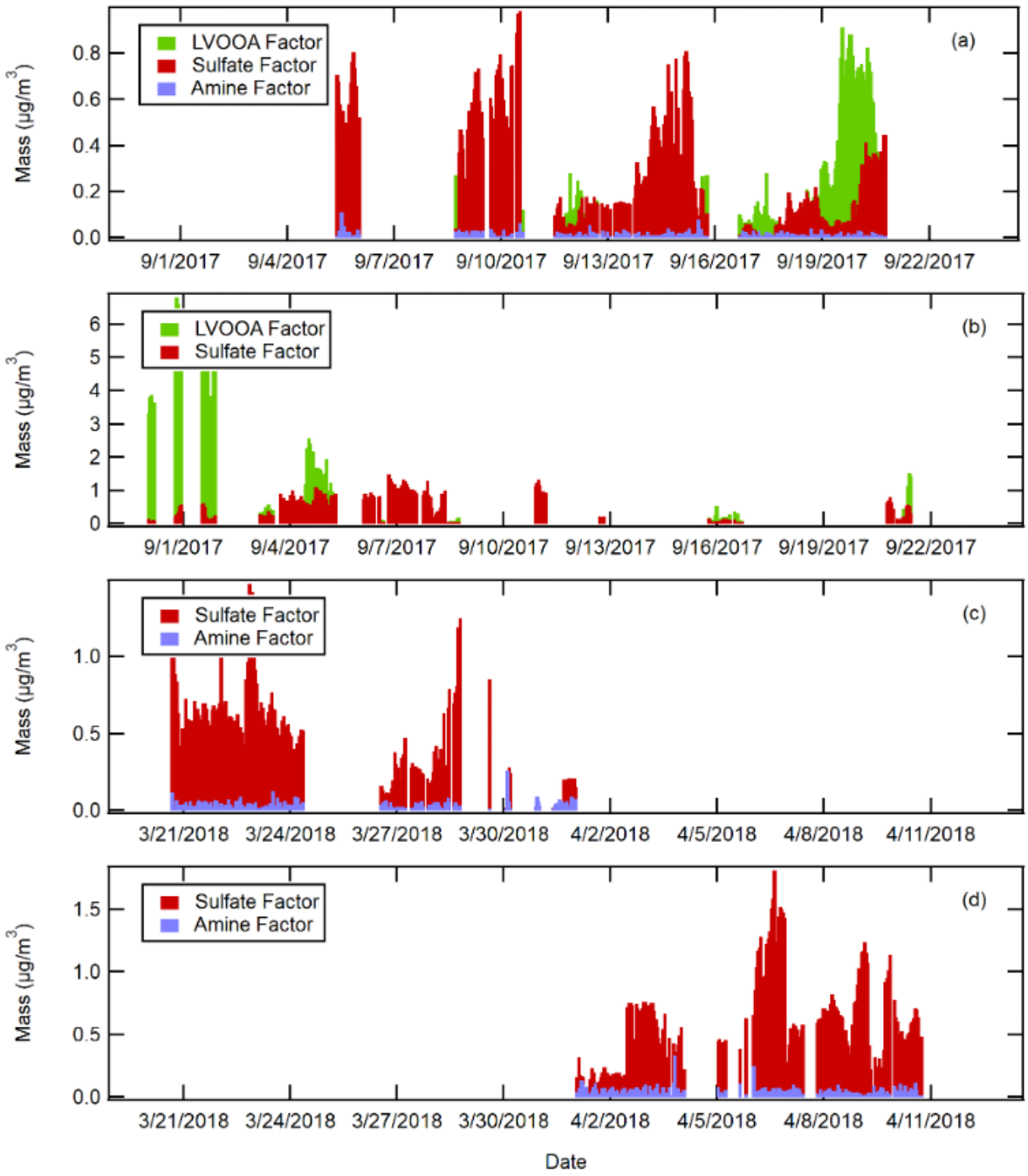

Figure S1. Time series (bottom right) of factors resolved from PMF analysis of AMS NR HR-Org and AMS NR HR-SO_4 for (a) marine air masses in Autumn, (b) continental air masses in Autumn, (c) marine air masses in Early Spring, and (d) continental air masses in Early Spring.

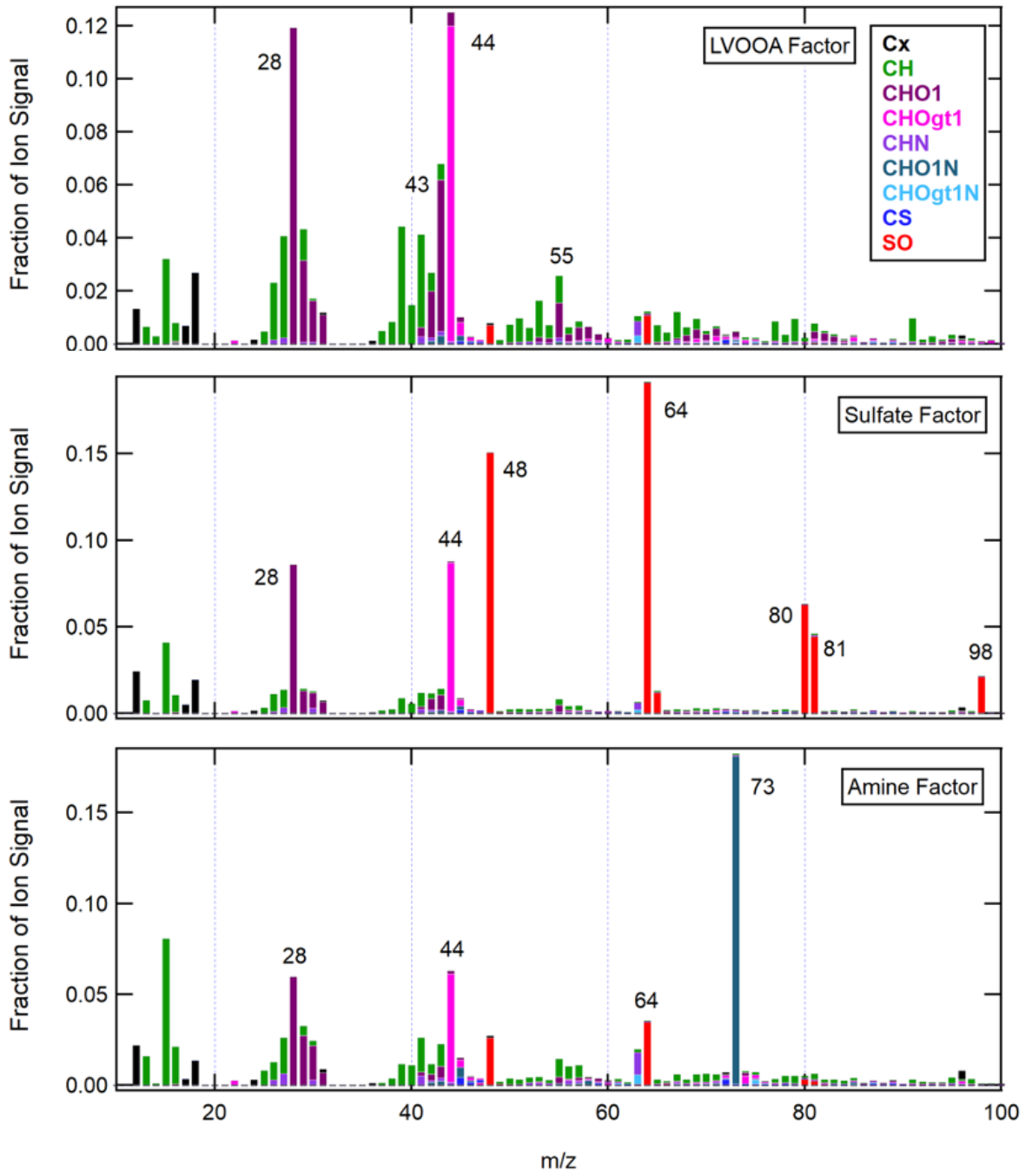

Figure S2. Mass spectra of factors resolved from PMF analysis of AMS NR HR-Org and AMS NR HR-SO_4 for marine air masses in Autumn. The factors shown include the LVOOA factor (top), the Sulfate factor (middle), and the Amine factor (bottom).

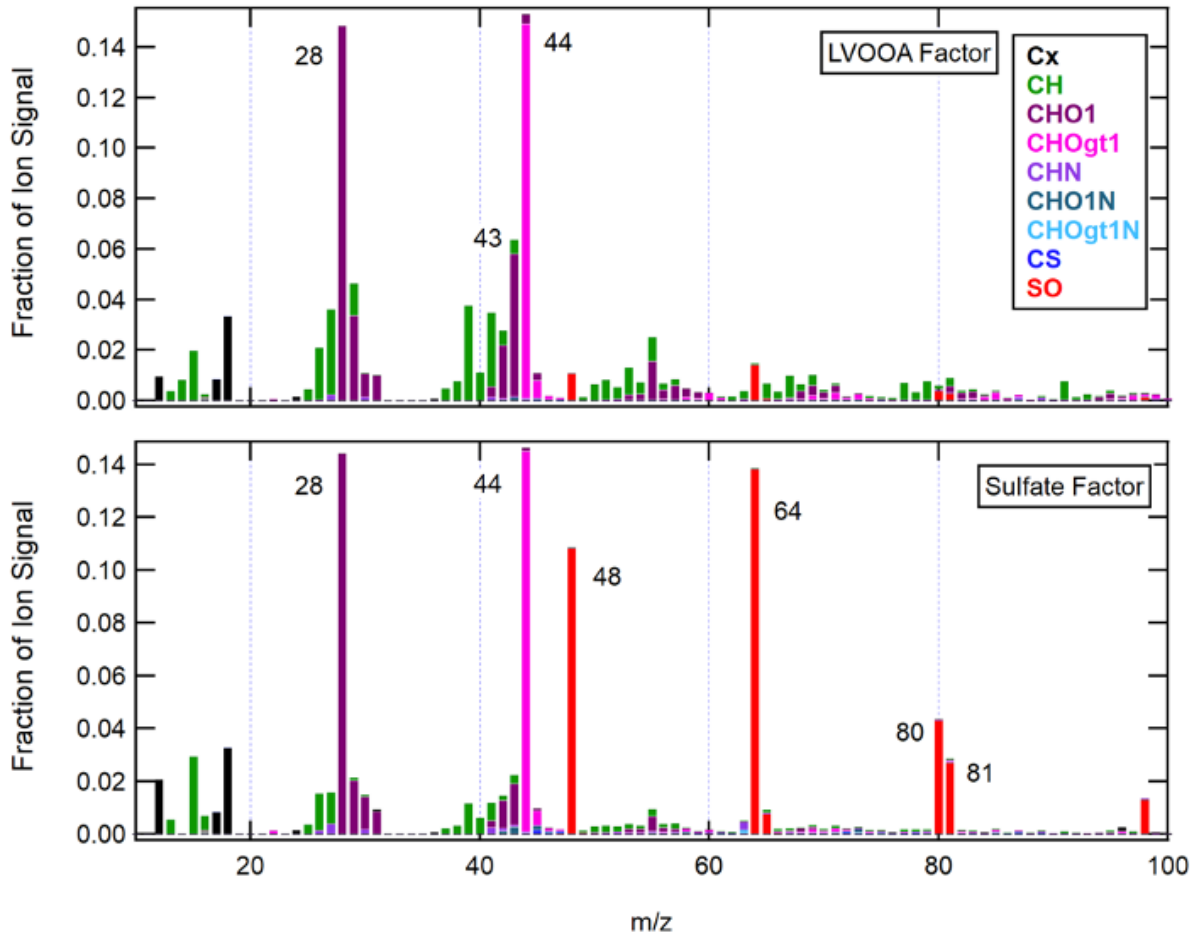

Figure S3. Mass spectra of factors resolved from PMF analysis of AMS NR HR-Org and AMS NR HR-SO_4 for continental air masses in Autumn. The factors shown include the LVOOA factor (top) and the Sulfate factor (bottom).

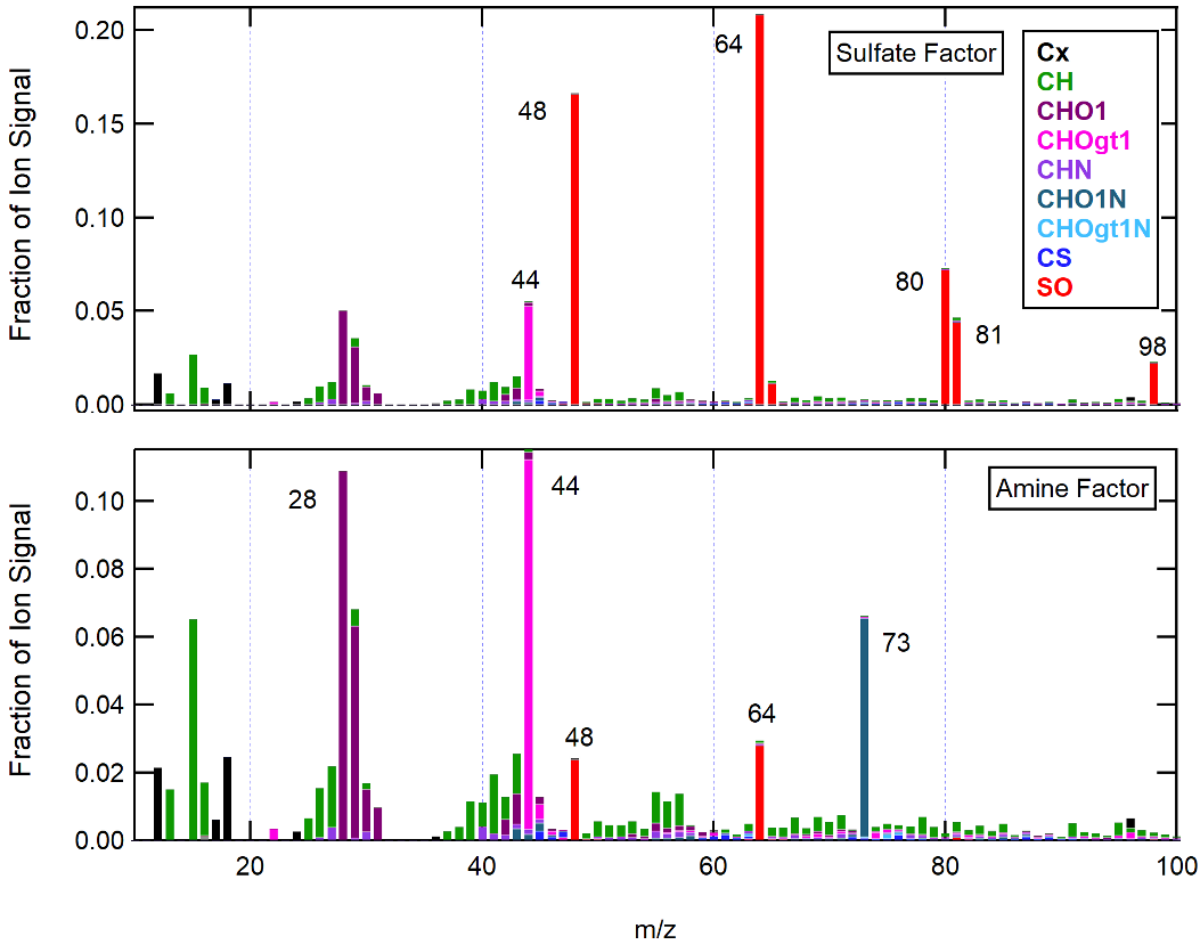

Figure S4. Mass spectra of factors resolved from AMS NR HR-Org and AMS NR HR-SO_4 for marine air masses in Early Spring. The factors shown include the Sulfate factor (top) and the Amine factor (bottom).

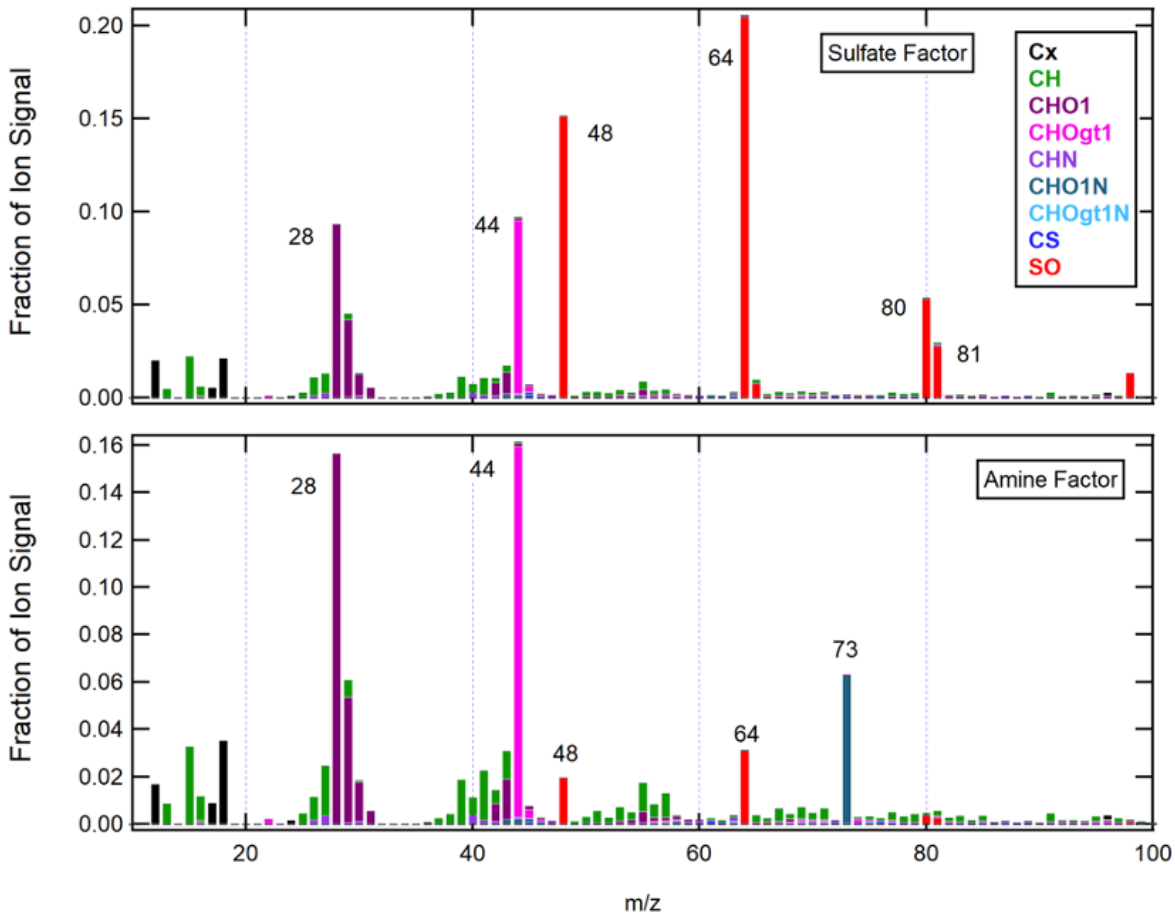

Figure S5. Mass spectra of factors resolved from PMF analysis of AMS NR HR-Org and AMS NR HR-SO_4 for continental air masses in Early Spring. The factors shown include the Sulfate factor (top) and the Amine factor (bottom).

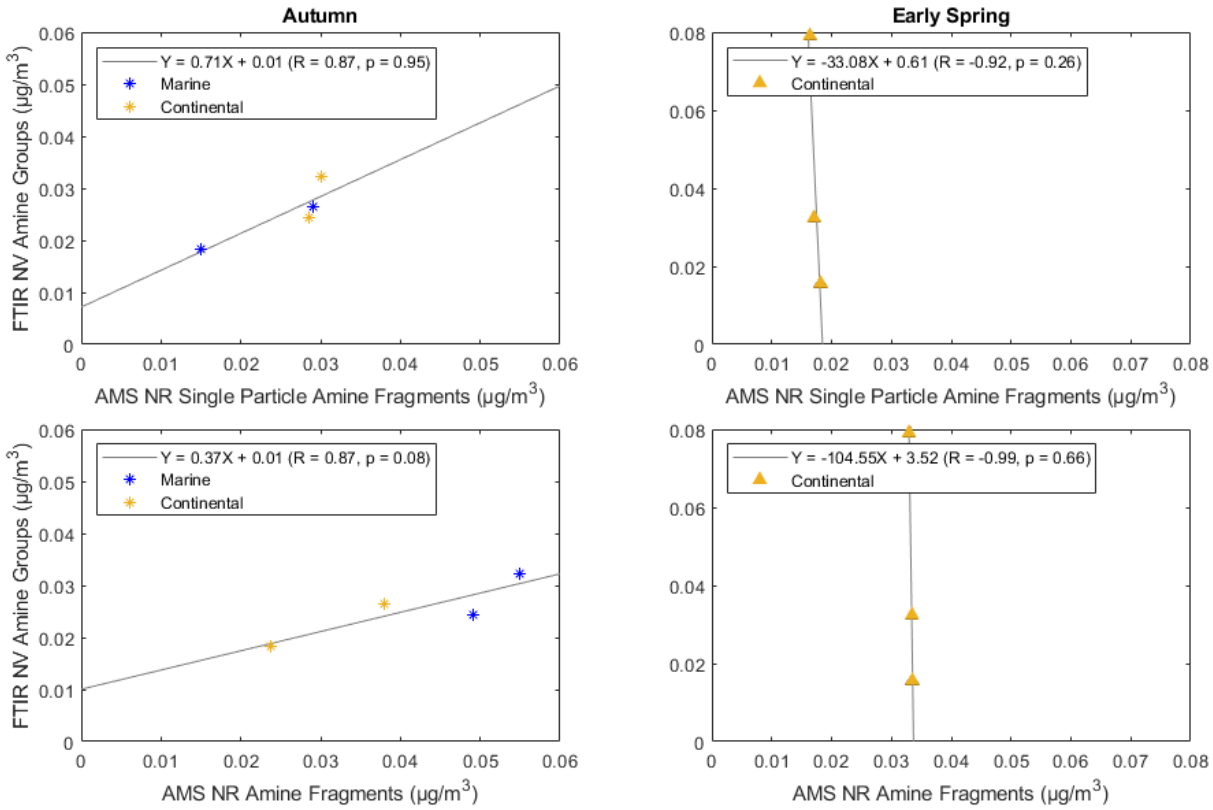

Figure S6. Scatter plot of FTIR (ADL) NV amine groups in particles with diameters <1 µm versus (top row) AMS NR single particle amine fragments and (bottom row) AMS NR amine fragments during (left column) Autumn and (right column) Early Spring. Marker colors represent air mass type (b,c): blue: marine, yellow: continental. The solid grey lines are the lines of best fit obtained using an ordinary least squares regression. A two-tailed T test is used to estimate p-values.

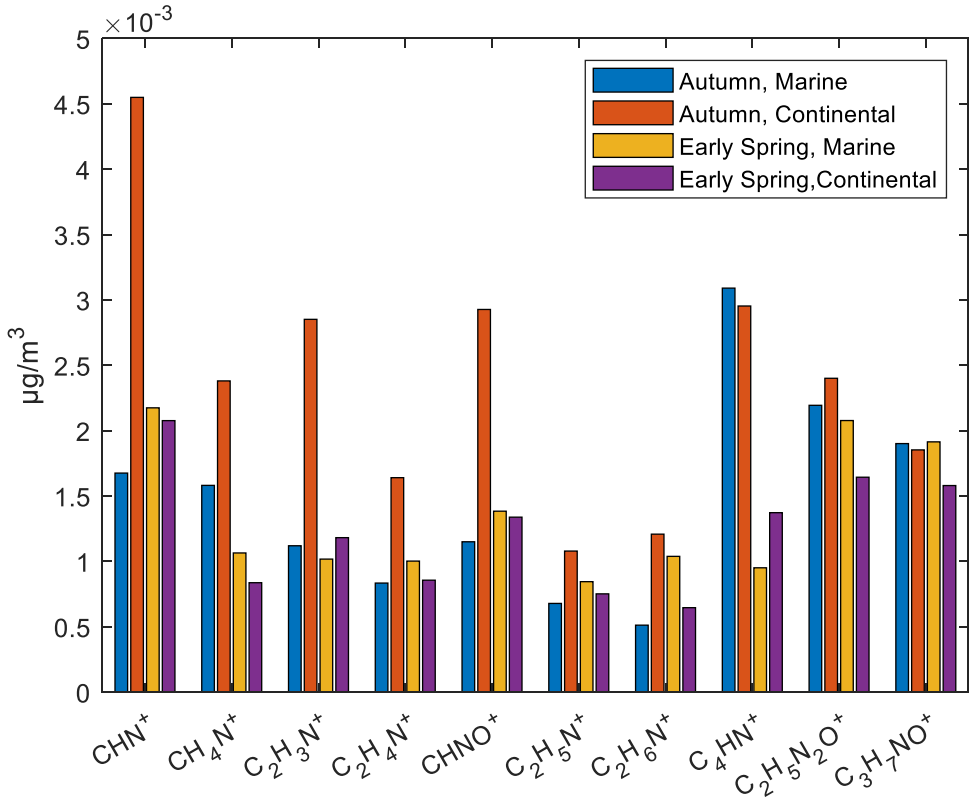

Figure S7. Bar graph of the 10 highest mass concentrations among AMS NR single particle amine fragments for marine air masses in Autumn (blue), continental air masses in Autumn (orange), marine air masses in Early Spring (yellow), and continental air masses in Early Spring (purple).

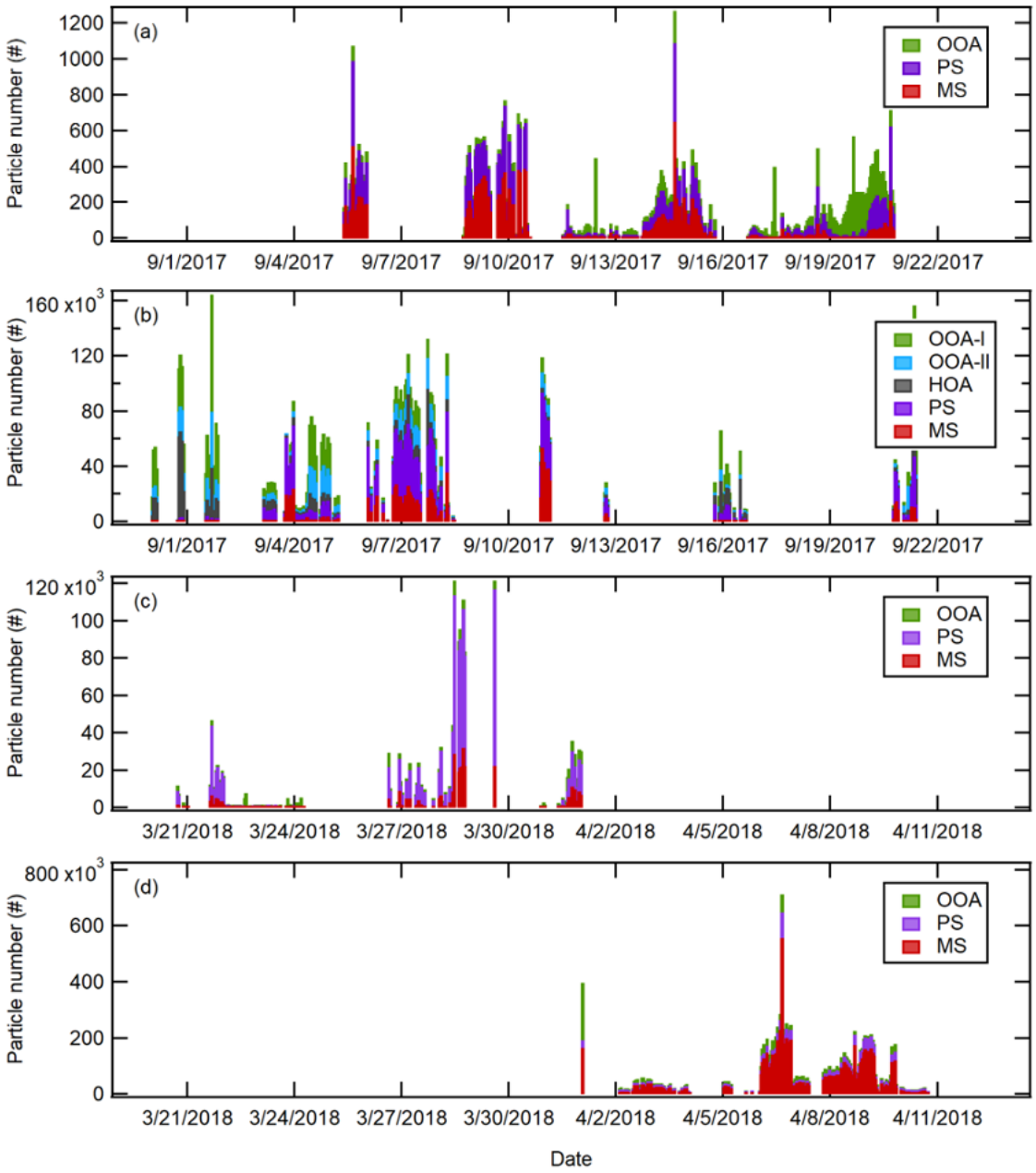

Figure S8. Time series of single particle clusters resolved from the ET mode for (a) marine air masses in Autumn, (b) continental air masses in Autumn, (c) marine air masses in Early Spring, and (d) continental air masses in Early Spring.

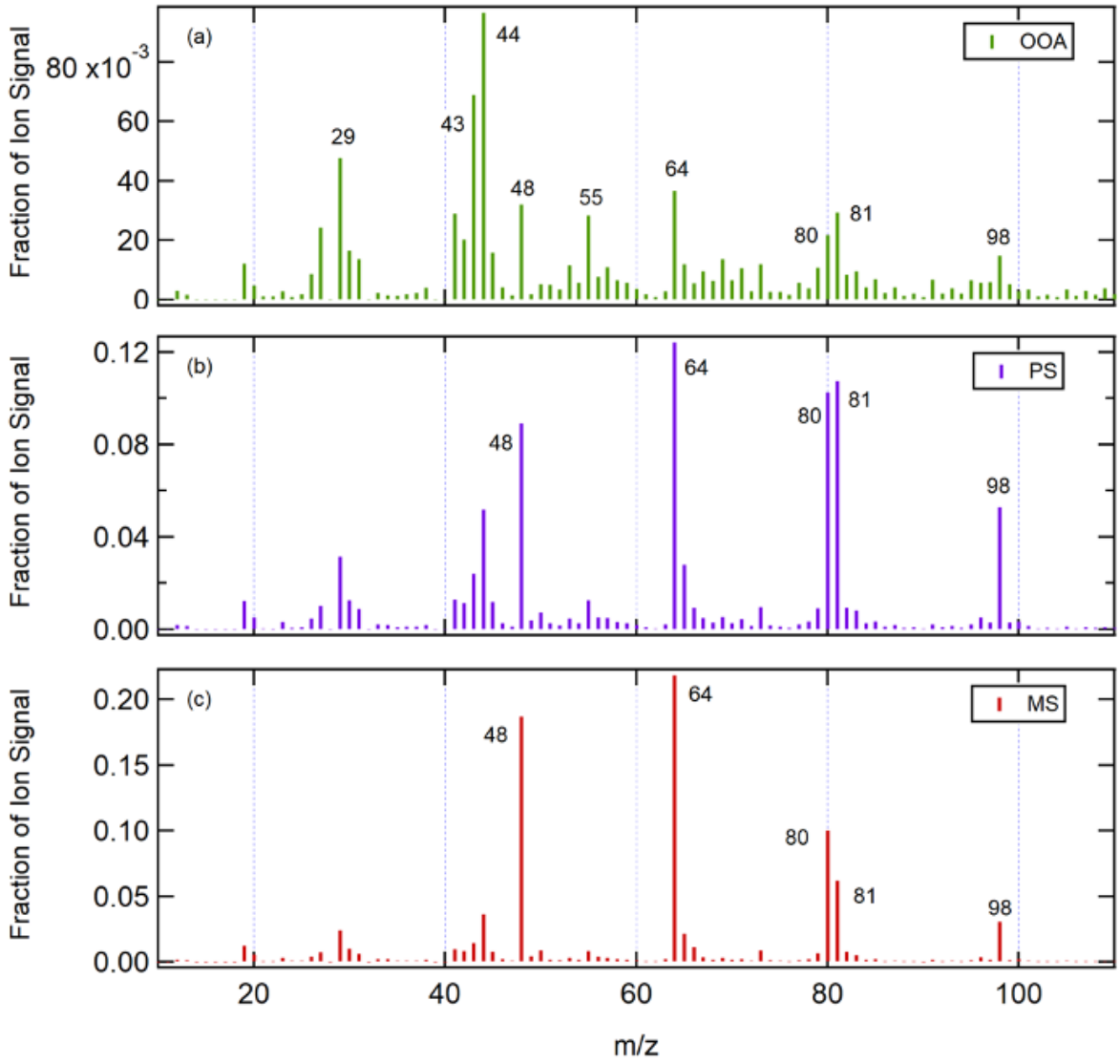

Figure S9. Mass spectra of single particle clusters resolved from the ET mode for marine air masses in Autumn. The particle types shown include (a) OOA, (b) PS, and (c) MS.

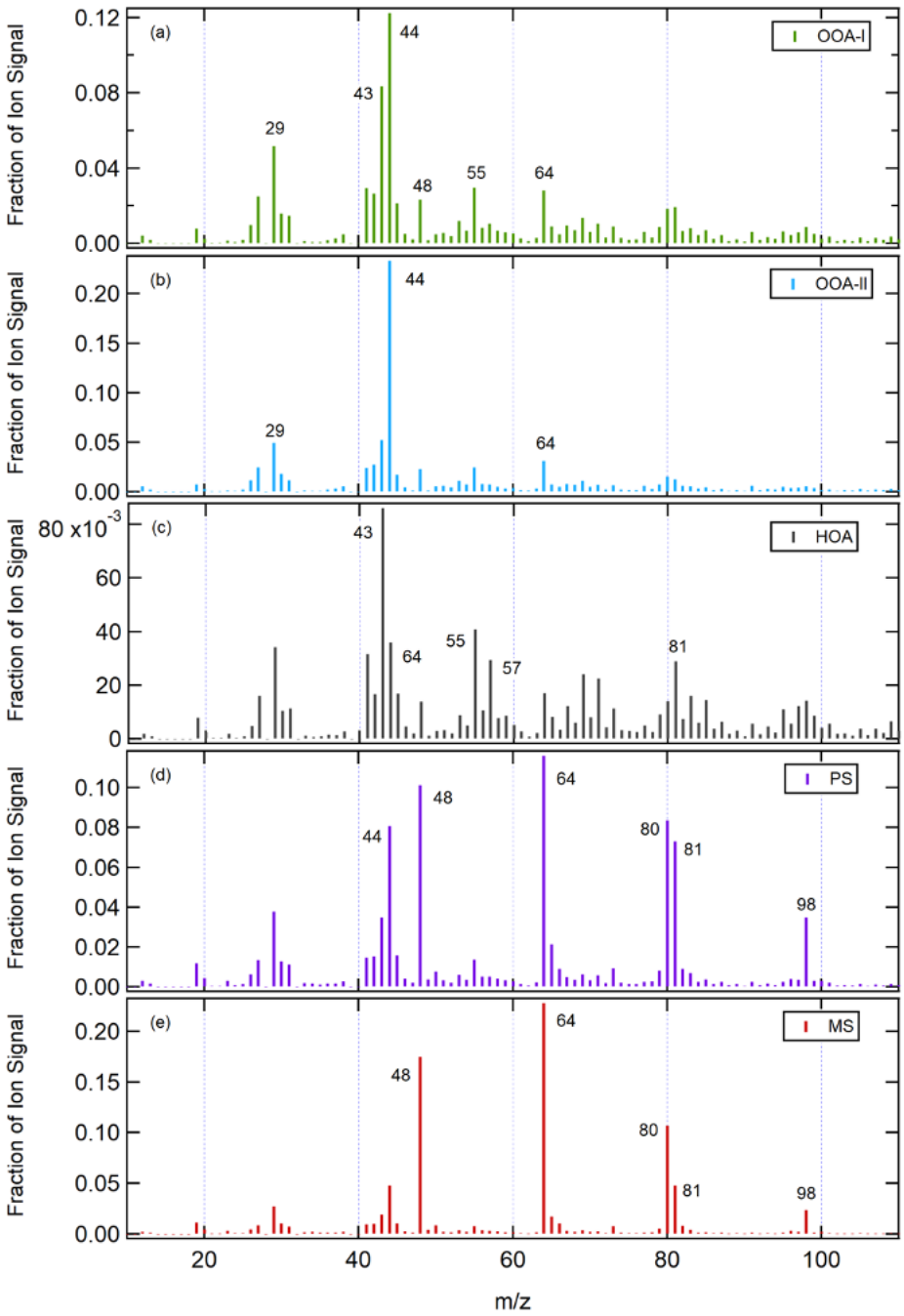

Figure S10. Mass spectra of single particle clusters resolved from the ET mode for continental air masses in Autumn. The particle types shown include (a) OOA-I, (b) OOA-II, (c) HOA, (d) PS, and (e) MS.

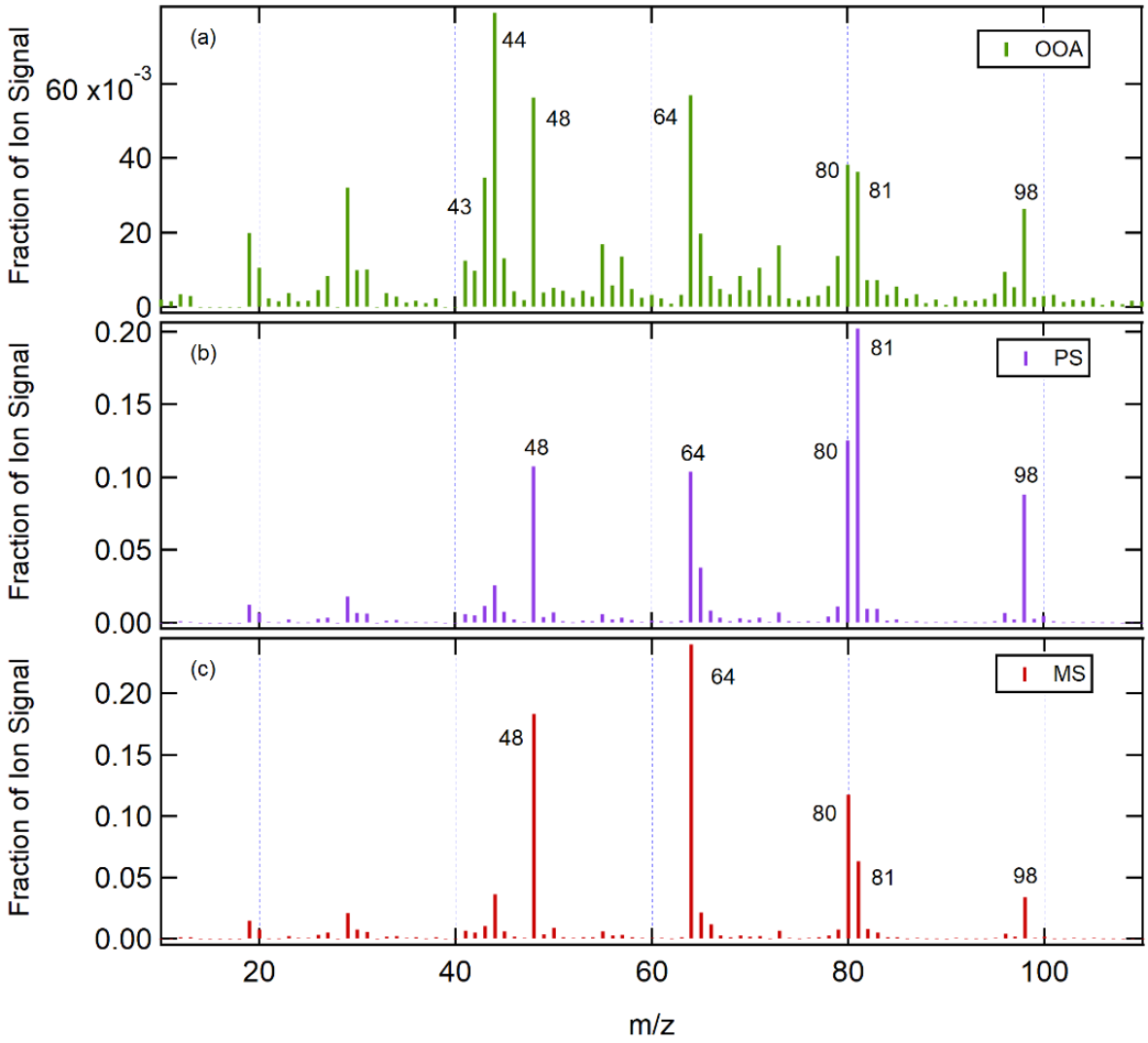

Figure S11. Mass spectra of single particle clusters resolved from the ET mode for marine air masses in Early Spring. The particle types shown include (a) OOA, (b) PS, and (c) MS.

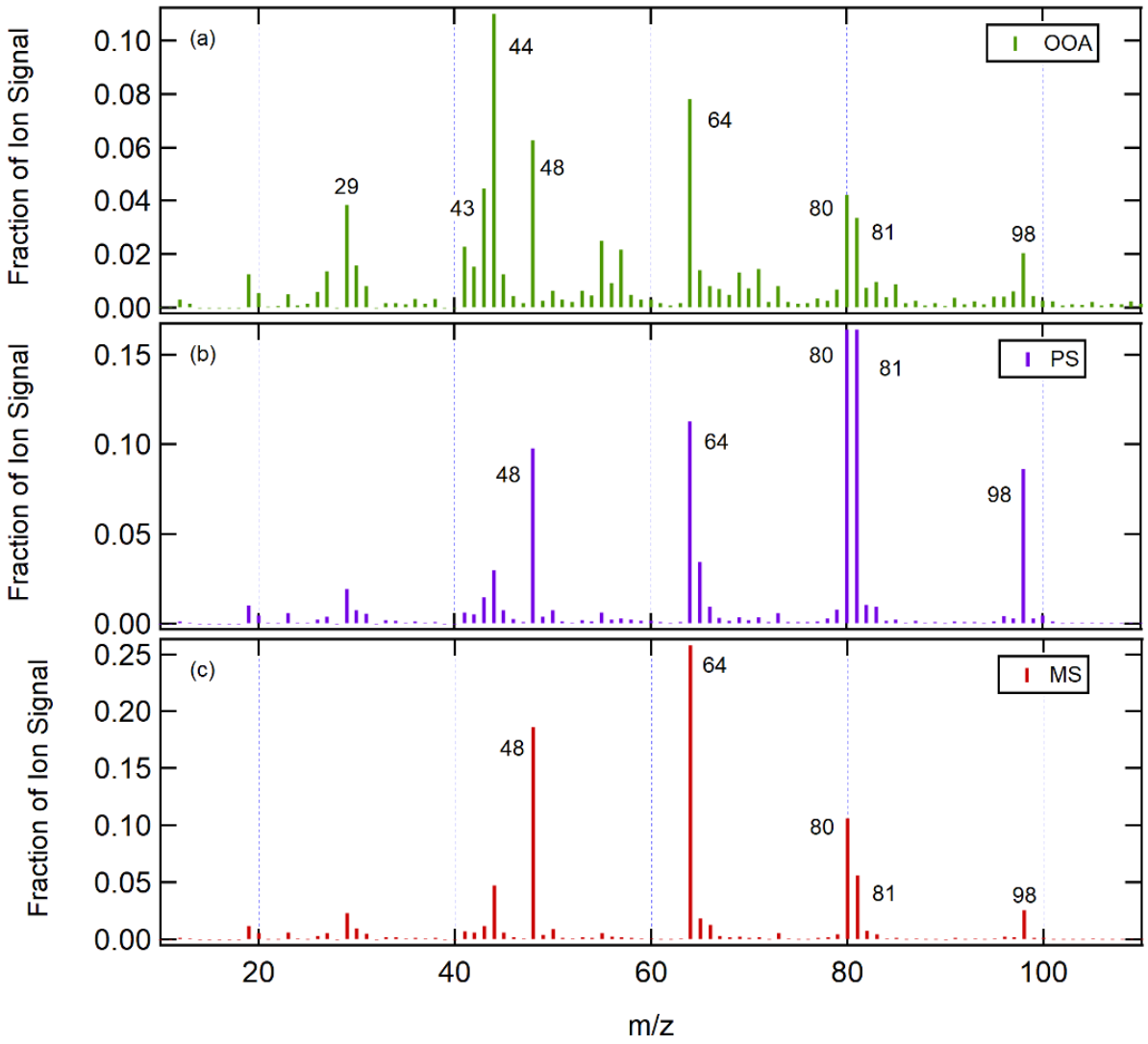

Figure S12. Mass spectra of single particle clusters resolved from the ET mode for continental air masses in Early Spring. The particle types shown include (a) OOA, (b) PS, and (c) MS.

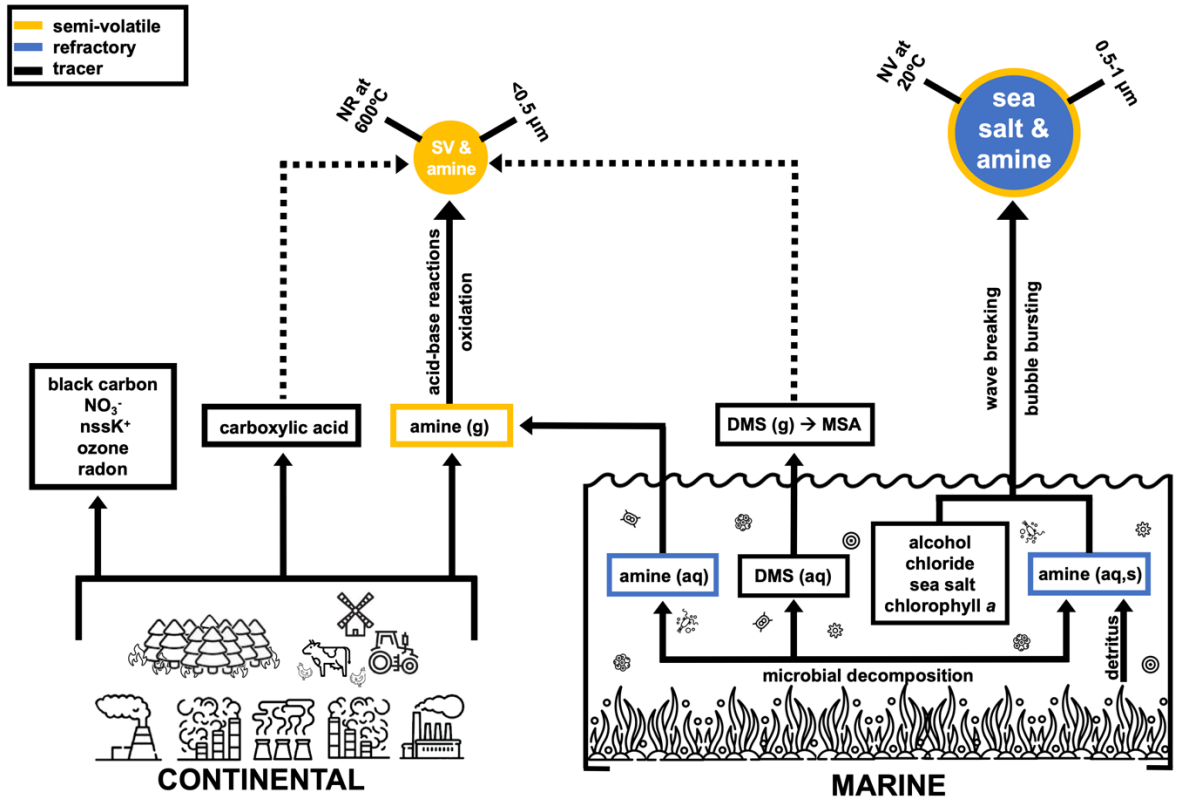

Figure S13. Diagram of tracers and amine sources in aerosols found in marine environments.

References.

Crippa, M., El Haddad, I., Slowik, J. G., DeCarlo, P. F., Mohr, C., Heringa, M. F., Chirico, R., Marchand, N., Sciare, J., Baltensperger, U., and Prevot, A. S. H.: Identification of marine and continental aerosol sources in Paris using high resolution aerosol mass spectrometry, Journal of Geophysical Research-Atmospheres, 118, 1950-1963, 10.1002/jgrd.50151, 2013.

Hayes, P. L., Ortega, A. M., Cubison, M. J., Froyd, K. D., Zhao, Y., Cliff, S. S., Hu, W. W., Toohey, D. W., Flynn, J. H., Lefer, B. L., Grossberg, N., Alvarez, S., Rappenglueck, B., Taylor, J. W., Allan, J. D., Holloway, J. S., Gilman, J. B., Kuster, W. C., De Gouw, J. A., Massoli, P., Zhang, X., Liu, J., Weber, R. J., Corrigan, A. L., Russell, L. M., Isaacman, G., Worton, D. R., Kreisberg, N. M., Goldstein, A. H., Thalman, R., Waxman, E. M., Volkamer, R., Lin, Y. H., Surratt, J. D., Kleindienst, T. E., Offenberg, J. H., Dusanter, S., Griffith, S., Stevens, P. S., Brioude, J., Angevine, W. M., and Jimenez, J. L.: Organic aerosol composition and sources in Pasadena, California, during the 2010 CalNex campaign, Journal of Geophysical Research-Atmospheres, 118, 9233-9257, 10.1002/jgrd.50530, 2013.

Hu, W. W., Hu, M., Yuan, B., Jimenez, J. L., Tang, Q., Peng, J. F., Hu, W., Shao, M., Wang, M., Zeng, L. M., Wu, Y. S., Gong, Z. H., Huang, X. F., and He, L. Y.: Insights on organic aerosol aging and the influence of coal combustion at a regional receptor site of central eastern China, Atmospheric Chemistry and Physics, 13, 10095-10112, 10.5194/acp-13-10095-2013, 2013.

Lee, A. K. Y., Willis, M. D., Healy, R. M., Onasch, T. B., and Abbatt, J. P. D.: Mixing state of carbonaceous aerosol in an urban environment: single particle characterization using the soot particle aerosol mass spectrometer (SP-AMS), Atmospheric Chemistry and Physics, 15, 1823-1841, 10.5194/acp-15-1823-2015, 2015.

Lee, A. K. Y., Rivellini, L. H., Chen, C. L., Liu, J., Price, D. J., Betha, R., Russell, L. M., Zhang, X. L., and Cappa, C. D.: Influences of Primary Emission and Secondary Coating Formation on the Particle Diversity and Mixing State of Black Carbon Particles, Environmental Science & Technology, 53, 9429-9438, 10.1021/acs.est.9b03064, 2019.

Ng, N. L., Canagaratna, M. R., Zhang, Q., Jimenez, J. L., Tian, J., Ulbrich, I. M., Kroll, J. H., Docherty, K. S., Chhabra, P. S., Bahreini, R., Murphy, S. M., Seinfeld, J. H., Hildebrandt, L., Donahue, N. M., DeCarlo, P. F., Lanz, V. A., Prevot, A. S. H., Dinar, E., Rudich, Y., and Worsnop, D. R.: Organic aerosol components observed in Northern Hemispheric datasets from Aerosol Mass Spectrometry, Atmospheric Chemistry and Physics, 10, 4625-4641, 10.5194/acp-10-4625-2010, 2010.

Petters, M. D., and Kreidenweis, S. M.: A single parameter representation of hygroscopic growth and cloud condensation nucleus activity, Atmospheric Chemistry and Physics, 7, 1961-1971, 10.5194/acp-7-1961-2007, 2007.

Qi, L., Bozzetti, C., Corbin, J. C., Daellenbach, K. R., El Haddad, I., Zhang, Q., Wang, J. F., Baltensperger, U., Prevot, A. S. H., Chen, M. D., Ge, X. L., and Slowik, J. G.: Source identification and characterization of organic nitrogen in atmospheric aerosols at a suburban site in China, Science of the Total Environment, 818, 10.1016/j.scitotenv.2021.151800, 2022.

Quinn, P. K., Bates, T. S., Coffman, D. J., Upchurch, L., Johnson, J. E., Moore, R., Ziemba, L., Bell, T. G., Saltzman, E. S., Graff, J., and Behrenfeld, M. J.: Seasonal Variations in Western North Atlantic Remote Marine Aerosol Properties, Journal of Geophysical Research-Atmospheres, 124, 14240-14261, 10.1029/2019jd031740, 2019.

Ulbrich, I. M., Canagaratna, M. R., Zhang, Q., Worsnop, D. R., and Jimenez, J. L.: Interpretation of organic components from Positive Matrix Factorization of aerosol mass spectrometric data, Atmospheric Chemistry and Physics, 9, 2891-2918, 10.5194/acp-9-2891-2009, 2009.